NIR LUMINESCENCE CHARACTERISTICS

OF Te-DOPED GLASSES

Penprapa Punpai

A Thesis Submitted in Partial Fulfillment of the Requirements for the

Degree of Master of Engineering in Ceramic Engineering

Suranaree University of Technology

Academic Year 2009

ลักษณะเฉพาะในการเปล่งแสงช่วงคลื่นอินฟราเรดใกล้ของแก้วที่เติมเทลลูเรียม

นางสาวเพ็ญประภา ผันผาย

วิทยานิพนธ์นี้เป็นส่วนหนึ่งของการศึกษาตามหลักสูตรปริญญาวิศวกรรมศาสตรมหาบัณฑิต
สาขาวิชาวิศวกรรมเซรามิก
มหาวิทยาลัยเทคโนโลยีสุรนารี
ปีการศึกษา 2552

NIR LUMINESCENCE CHARACTERISTICS

OF Te-DOPED GLASSES

Suranaree University of Technology has approved this thesis submitted in partial fulfillment of the requirements for a Master's Degree.

Thesis Examining Committee

_____

(Assoc. Prof. Dr. Sutin Kuharuangrong)

Chairperson

_____

(Assoc. Prof. Dr. Shigeki Morimoto)

Member (Thesis Advisor)

_____

(Dr. Veerayuth Lorprayoon)

Member

_____   _____

(Prof. Dr. Sukit Limpijumnong)   (Assoc. Prof. Dr. Vorapot Khompis)

Vice Rector for Academic Affairs   Dean of Institute of Engineering

เพ็ญประภา ผันผาย : ลักษณะเฉพาะในการเปล่งแสงช่วงคลื่นอินฟราเรดใกล้ของแก้ว
ที่เติมเทลลูเรียม (NIR LUMINESCENCE CHARACTERISTICS OF Te-DOPED
GLASSES) อาจารย์ที่ปรึกษา : รองศาสตราจารย์ ดร.ชิเกกิ โมริโมโต, 98 หน้า.

การศึกษาศูนย์กลางสี ศูนย์กลางการเปล่งแสงช่วงคลื่นอินฟราเรดใกล้ (Near Infrared)
และลักษณะเฉพาะในการเปล่งแสงช่วงคลื่นอินฟราเรดใกล้ของแก้วที่มีเทลลูเรียม ตามหลักสมดุล
ของปฏิกิริยารีดอกซ์ โดยการศึกษาความสัมพันธ์ระหว่างระดับชั้นวาเลนซ์และปัจจัยที่มีผลต่อสม
ดุลของปฏิกิริยารีดอกซ์ ได้แก่ อุณหภูมิในการหลอม ส่วนผสม ปริมาณของเทลลูเรียม และคาร์บอน
ซึ่งเป็นสารช่วยรีดิวส์ ในแก้วบอเรตและแก้วโซดาไลม์ซิลิเกตที่มีเทลลูเรียม รวมถึงการศึกษาโครง
สร้างและคุณสมบัติของแก้วบอเรตที่เติมเทลลูเรียมด้วย

การศึกษาพบว่าสมดุลของปฏิกิริยารีดอกซ์มีผลอย่างมากต่อการเกิดศูนย์กลางสี ศูนย์กลาง
การเปล่งแสงช่วงคลื่นอินฟราเรดใกล้ และลักษณะเฉพาะในการเปล่งแสงของแก้วที่เติมเทลลูเรียม
ในสภาวะออกซิไดซ์ ศูนย์กลางสีและศูนย์กลางการเปล่งแสงช่วงคลื่นอินฟราเรดใกล้จะไม่เกิดขึ้น
ทำให้การเปล่งแสงช่วงคลื่นอินฟราเรดใกล้ไม่สามารถตรวจพบได้ ในสภาวะรีดิวส์สูง แก้วมีสีน้ำ
ตาลดำ และเกิดการรวมตัวกันกลายปืนคอลลอยด์ของโลหะเทลลูเรียมในเนื้อแก้วบอเรต
และไม่พบการเปล่งแสงช่วงคลื่นอินฟราเรดใกล้

ในแก้วโซดาไลม์ซิลิเกต ไม่พบกระบวนการเกิดคอลลอยด์ของโลหะเทลลูเรียม เนื่องจาก
ปริมาณความเข้มข้นของเทลลูเรียมไดออกไซด์ในแก้วโซดาไลม์ซิลิเกตมีปริมาณน้อยเพียง 1.0%
โดยน้ำหนัก ส่วนในแก้วบอเรตมี 19.0% โดยน้ำหนัก ดังนั้นคาร์บอนจึงรีดิวส์เทลลูเรียมไดออกไซด์
เป็นเทลลูเรียมอะตอมหรือโมเลกุล เมื่อความเข้มข้นของโมเลกุลเหล่านี้สูงขึ้นจึงรวมตัวกัน
และกลายเป็นคอลลอยด์ของโลหะเทลลูเรียมในแก้วบอเรต เมื่อเทียบกับความเข้มข้นของเทลลูเรียม
อะตอมหรือโมเลกุลในแก้วโซดาไลม์ซิลิเกตซึ่งต่ำกว่าแก้วบอเรต จึงไม่พบกระบวนการเกิดคอล
ลอยด์ของโลหะเทลลูเรียม

นอกจากนี้เป็นที่สังเกตว่าอัตราส่วนระหว่าง C/TeO_2 มีผลต่อการก่อตัวของศูนย์กลาง
การเปล่งแสง อัตราส่วนที่เหมาะสมระหว่าง C/TeO_2 เท่ากับ 0.3 สำหรับความเข้มข้นสูงสุดในการ
เปล่งแสงช่วงคลื่นอินฟราเรดใกล้ของแก้วโซดาไลม์ซิลิเกตที่มีเทลลูเรียม ดังนั้นในแก้วโซดาไลม์
ซิลิเกต ศูนย์กลางสีและศูนย์กลางการเปล่งแสงช่วงคลื่นอินฟราเรดใกล้เกิดจาก Te_2^{-} และปรากฏ
แถบดูดกลืน และการเปล่งแสงในช่วงคลื่นอินฟราเรดใกล้อยู่ที่ประมาณ 630 และ 1200 นาโนเมตร
ตามลำดับ

สาขาวิชา <u>วิศวกรรมเซรามิก</u>   ลายมือชื่อนักศึกษา_____

ปีการศึกษา 2552   ลายมือชื่ออาจารย์ที่ปรึกษา_____

PENPRAPA PUNPAI : NIR LUMINESCENCE CHARACTERISTICS OF Te-DOPED GLASSES. THESIS ADVISOR : ASSOC. PROF. SHIGEKI MORIMOTO, Ph.D., 98 PP.

TELLURIUM OXIDE/NEAR INFRARED LUMINESCENCE/COLOR CENTER/ LUMINESCENCE CENTER/REDOX EQUILIBRIUM

The color center, near-infrared (NIR) luminescent center and NIR luminescence characteristics of Te-doped glasses were investigated based on redox equilibrium. The relationship between the valence state and the factors affecting the redox equilibrium i.e. melting temperature, glass composition, Te concentration and addition of carbon as a reducing agent were investigated in Te-containing borate glasses and soda-lime-silicate glasses. In addition, structure and properties of Te-containing borate glasses were studied.

It was found that the formation of color center and NIR luminescent center and luminescent characteristic of Te- containing glasses were strongly affected by redox equilibrium. In oxidizing condition, color center and NIR luminescent center were not formed, and hence NIR luminescence could not be detected. In strongly reducing condition, glasses appear to be brown to black color and finally Te metal colloids deposited in borate glasses and also NIR luminescence was not observed.

In soda-lime-silicate glass, the formation process of Te metallic colloids was not observed due to low concentration of 1.0 wt% TeO_2 in soda-lime-silicate glass as compared to 19 wt% in borate glass. Thus, carbon reduces TeO_2 to Te atoms or molecules, the concentration of these species becomes to be high and they gather together, grow and form Te metallic colloids in borate glass. It is considered that the

concentration of the Te atoms or molecules in soda-lime-silicate glass is lower than borate glass and hence the formation process of Te metallic colloids was not observed. Furthermore, it is noted that the C/TeO_2 ratio also affects the formation of luminescent center, the optimum ratio of C/TeO_2 is 0.3 for maximum NIR luminescent intensity of TeO_2 doped soda-lime-silicate glass.

Consequently, in soda-lime-silicate glass, the color center and NIR luminescent center were formed by Te_2^- and the absorption band and NIR luminescence appear at around 630 nm and 1200 nm, respectively.

School of <u>Ceramic Engineering</u>   Student's Signature _____

Academic Year 2009   Advisor's Signature _____

ACKNOWLEDGEMENTS

TABLE OF CONTENTS

PAGE

TABLE OF CONTENTS (Continued)

TABLE OF CONTENTS (Continued)

TABLE OF CONTENTS (Continued)

TABLE OF CONTENTS (Continued)

TABLE OF CONTENTS (Continued)

TABLE OF CONTENTS (Continued)

LIST OF TABLES

LIST OF FIGURES

LIST OF FIGURES (Continued)

LIST OF FIGURES (Continued)

FIGURE   **PAGE**

CHAPTER I

INTRODUCTION

Owing to rapid increase of information traffic in the telecommunication network, the development of wavelength-division-multiplexing (WDM) network system becomes important. WDM point-to-point systems provide very large capacity between widely spaced (300 to 600 km) end terminals, in many networks it is necessary to drop some traffic and decrease the capacity of process (Trigg, 2006). Therefore, devices for the WDM optical communication system, such as amplifiers and tunable lasers, an optical amplifier is a device that amplifies an optical signal directly, without the need to first convert it to an electrical signal. The signal is to be amplified and a pump laser is multiplexed into the doped fibre, and the signal is amplified through interaction with the doping ions. Amplification is achieved by stimulated emission of photons from dopant ions in the doped fibre as shown in Figture 1.1. The pump laser excites ions into a higher energy level from where they can decay via stimulated emission of a photon at the signal wavelength back to a lower energy level. The excited ions can also decay spontaneously (spontaneous emission) or even through nonradiative processes involving interactions with phonons of the glass matrix. Optical amplifiers and tunable lasers should be key materials, because the number of channels depends on the gain bandwidth (the gain is dependent on wavelength) of the amplifiers and tunable laser source. In order to develop broadband amplifiers and tunable laser sources for the efficient WDM system, it

gradually becomes important to explore and synthesize new luminescent materials with larger FWHM (full widths at half maximum) emission in the telecommunication wavelength region, to fully utilize the wide window of silica glass fiber in the range of 1.26-1.675 μm (NIR) (Ren et al., 2007). Considerable efforts have been devoted to rare earth ions- and transition metal ions-doped materials.
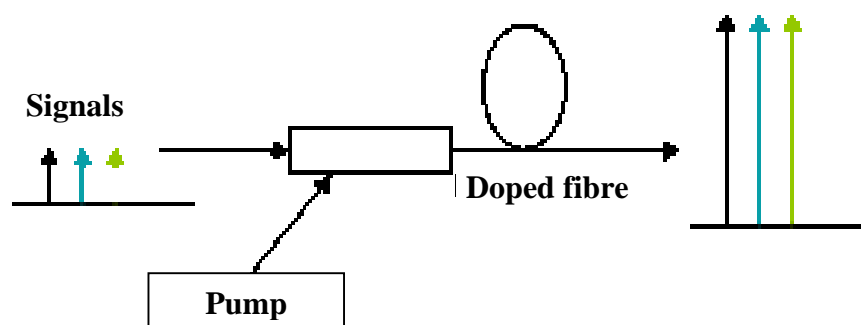
Figture 1.1 Schematic diagram of a simple Doped Fibre Amplifier

(Wikipedia, www, 2008).

Many attempts have been made on broadening and flattening of gain spectra of optical fiber amplifiers such as Er^{3+}-doped fiber amplifiers (EDFAs), which has broadband light source operating in the 1.55 μm telecommunication band (Wikipedia, www, 2008). Tm^{3+}-doped fiber amplifiers (TDFAs) are operating in the range of 1.45-1.50 μm (Sakamoto et al., 1995). Broadband tunable lasers, such as $Ti^{3+}:Al_2O_3$ (sapphire), is the most widely used crystal for wavelengths tunable lasers and can be lased over the entire band from 600 to 1100 nm (VIS-NIR region) (Albrecht, Eggleston, and Ewing, 1985), $Cr^{4+}: Y_3Al_5O_{12}$ (YAG) shows the output in the 1.2-1.5 μm (NIR region) at room temperature (Sorokina, Naumov, Sorokin, Wintner, and Shestakov, 1999), $Cr^{4+}: MgSiO_4$ crystal can generate near infrared emission at

1.2-1.6 μm (Perceives, Gayen, and Alfano, 1988) and were realized by using transition metal ions as active ions. The Ni^{2+} ion-doped Spinel transparent glass-ceramics is also promising materials as broad band near infrared tunable lasers (Suzuki, Murugan, and Ohishi, 2005; Khonthon, Morimoto, and Ohishi, 2006). The consideration of many research as mentioned previously, already show that NIR luminescence materials are important and use for the optical network and many researchers are still interested and finding for new NIR luminescence materials, clearly known of the origin and characteristics of luminescence materials, possibly to be discovery of new NIR amplifiers and NIR tunable laser materials, as shown in Table 1.1.

Table 1.1 Common laser-active rare earth ions and host media and important

emission wavelength regions (rp-photonics, www, 2008).

Ion	Common host media	Important emission region
Erbium (Er^{3+})	YAG, silica[I]	1.55-1.6 μm, 2.7 μm, 0.55 μm
Thulium (Tm^{3+})	YAG, silica, ZBLYAN[II], fluoride gasses	1.7-2.1 μm, 1.45-1.50 μm, 0.48 μm, 0.8 μm
Neodymium (Nd^{3+})	YAG, YVO4[III], YLF, silica	1.0-1.1 μm, 0.9-0.95 μm, 1.32-1.35 μm
Ytterbium (Yb^{3+})	YAG, tungstates, silica	1.0-1.1 μm
Praseodymium (Pr^{3+})	silica, fluoride glasses, Ge-Ga-S glasses[IV]	1.3 μm, 0.635 μm, 0.6 μm, 0.52 μm, 0.49 μm

Remarks: [I] Wikipedia, www, (2008), [II] Sakamoto et al., (1995),

[III] Li, Wu, and Song, (2008), [IV] Park, Heo, and Kim, (1999)

Generally, the luminescence is the phenomenon in which the materials absorb the energy and emits UV-VIS and NIR light subsequently. In this process, the absorption center (color center) is regarded also as luminescent center. Luminescence is due to the addition of a luminogen or activator in the form of a trace impurity such as transition metal or rare earth ions. In some case crystal lattice defects provide localized level, like those of impurity, which play the part of the activator (Curie, 1963).

The glass coloration in visible region is usually induced by impurities, such as transition metal ions, rare earth ions or nanometer sized semiconductor and metal particles. There are numerous other sources of visible coloration in glasses which are of interest. Included in this group are blue-sulfur (S), pink-selenium (Se), and purple or green-tellurium (Te) glasses whose colors are associated with elemental clustering (Sigel, 1977). The finding from elemental clustering reveals that the luminescence from sulfur was found in UV-VIS region but not in NIR region and color centers are S_2, S_2^- (Ahmed, Sharaf, and Codreate, 1997). Selenium has similar luminescent characteristics to sulfur and the color centers are Se_2, Se_2^- (Paul, 1975; Guha, Leppert, and Risbud, 1998). Tellurium was found to have a luminescence in UV-VIS region but no information in the NIR region and the color centers are Te_2, Te_2^- (Lindner, Witke, Schlaich, and Reinen, 1996; Konishi et al., 2003).

The high TeO_2 containing glasses are promising candidate for photonic device applications, because of their special properties; wide transmission window, good glass stability and durability, high refractive index, large non-linear optical sensibility, relatively low phonon energy in blue (Lee, Kim, Park, Chung, and Chang, 1991) and green band emission (Kishino, Tanaka, Senda, Yamada, and Taguchi, 2000) region.

The broadband erbium-doped fiber amplifiers have been demonstrated using TeO_2-based glass fibers as host materials (Ohishi et al., 1998).

However, high TeO_2 containing glasses often show the pale green to brilliant purple coloration depending on glass compositions and melting conditions, the color centers of these glasses have already been reported that the color center of pale green TeO_2- containing glasses is Te clusters; Te_2 and Te_2^-, and that of brilliant purple is Te metallic colloids (Konishi et al., 2003). The valence state of ions in glasses could be explained by redox equilibrium, which depends upon the melting temperature and time, the glass composition, the furnace atmosphere and the batch composition (Paul, 1990).

In the past, some researches on the luminescence properties in UV-VIS region of Te-doped crystals have been done but not in NIR region (Pal, Fernandez, and Piqueras, 1995; Garcia, Ramons, Munoz, and Triboulet, 1998). Recently, however, Khonthon et al., (2007, 2008) have found the NIR luminescence centered at 1250 nm with a half width of 250 nm from pale green and purple TeO_2-containing glasses and glass-ceramics which are discovered for the first time. Although, the color center of Te-doped glasses and crystals has already been identified, the NIR luminescent center of Te-doped glasses is not clear yet.

Therefore, this research focuses on the NIR luminescence characteristics of Te-doped glasses in relation to valence state and preparation conditions.

1.1   Research objective

The objectives of this research are to focus on the relationship between the change in valence state and accompanying optical properties such as the formation of

color center and luminescent center of TeO_2 containing glass.

1. To investigate the relationship between valence state of Te ions and preparation conditions.

2. To determine the factors affecting on NIR luminescence of Te-doped glasses. (Melting temperature, Glass composition, Carbon addition and TeO_2 concentration)

Experimental subject

I. Preliminary Research

Identification of color center and NIR luminescence center of Te-doped soda-lime-silicate and borate glasses.

II. Fundamental research

Investigation of factors affecting on valence state and NIR luminescence of Te- doped soda-lime-silicate and borate glasses.

1. **Te-Borate glasses;**

a) Melting temperature

- Glass composition: $63B_2O_3.9Al_2O_3.9ZnO.9K_2O.10TeO_2$ (mol%)

- Melting temperature: 850, 1000, 1100, 1200 and 1300°C for

15-60 min

- Annealing temperature: 450°C for 30 min

b) Glass composition

- Glass compositions: $90[(80-X)B_2O_3.10Al_2O_3.10ZnO.XK_2O]$

$10TeO_2$ (mol%, X=0, 10, 20 and 30)

- Melting temperature: 1200°C for 15-60 min

- Annealing temperature: 450°C for 30 min

c) Carbon addition

- Glass composition: $63B_2O_3.9Al_2O_3.9ZnO.9K_2O.10TeO_2$ (mol%). XCarbon (X=0, 0.5 and 1, wt%)

- Melting temperature: 1000°C for 15-60 min

- Annealing temperature: 450°C for 30 min

d) Structure and properties of TeO_2- containing borate glasses

- Glass composition: $(100-X)[80B_2O_3 \cdot 10Al_2O_3 \cdot 10ZnO] \cdot XTeO_2$ (mol%,X=0, 10, 20 and 30)

- Melting temperature: 1000-1200°C for 30 min

- Annealing temperature: 400-500°C for 30 min

2. **Te-doped soda-lime-silicate;**

a) Carbon addition

- Glass composition: $72SiO_2 \cdot 2Al_2O_3 \cdot 4MgO \cdot 8CaO \cdot 13Na_2O \cdot 1K_2O \cdot 1TeO_2 \cdot Xcarbon$ (wt %, X=0, 0.1, 0.2, 0.3, 0.5 and 1).

- Melting temperature: 1450°C for 60 min

- Annealing temperature: 600˚C for 30 min

b) TeO_2 concentration

- Glass composition: $72SiO_2 \cdot 2Al_2O_3 \cdot 4MgO \cdot 8CaO \cdot 13Na_2O \cdot 1K_2O \cdot XTeO_2 \cdot 0.3carbon$ (X=0.2, 0.5, 0.7, 1.0 and 2.0wt %).

- Melting temperature: 1450°C for 60 min

- Annealing temperature: 600˚C for 30 min

1.2   Scope and limitation of research

1. Investigation of UV-VIS and NIR luminescence characteristics of Te-clustersin glasses

2. Investigation of formation of color center and NIR luminescence center of Te-doped glasses based on redox reaction

1.3   Expected results

1. Establishment of basic technology for the preparation of elemental clustering of Te-doped glasses

2. Identification of color center and luminescent center of Te-doped glasses

3. Discovery of new NIR amplifiers and NIR tunable laser materials

CHAPTER II

LITERATURE REVIEW

2.1   Glasses system

2.1.1 Soda-lime glass

Pure silica (SiO_2) has a glass melting point at a viscosity of 10 Pa·s (100 P) of over 2300°C . While pure silica can be made into glass for special applications, other substances are added to common glass to simplify processing. One is sodium carbonate (Na_2CO_3), which lowers the melting point to about 1500°C in soda-lime glass; "soda" refers to the original source of sodium carbonate in the soda ash obtained from certain plants. However, the soda makes the glass water soluble, which is usually undesirable, so lime (calcium oxide (CaO), generally obtained from limestone), some magnesium oxide (MgO) and aluminum oxide (Al_2O_3) are added to provide for a better chemical durability. The resulting glass contains about 70 to 74 percent silica by weight and is called a soda-lime glass (Wikipedia, www, 2009).

Soda-lime glass or soda-lime-silicate glass is perhaps the least expensive and the most widely used of all glasses made commercially. Most of the beverage containers, glass windows, and incandescent and fluorescent lamp envelopes are made from soda-lime glass. It has good chemical durability, high electrical resistivity, and good spectral transmission in the visible region. Because of its relatively high coefficient of thermal expansion ($\sim100\times10^{-7}$/°C), it is prone to thermal shock failure, and this prevents its use in a number of applications. Large scale

continuous melting of inexpensive batch materials such as soda ash (Na_2CO_3), limestone ($CaCO_3$) and sand at 1400-1500°C make it possible to form the products at high speeds inexpensively (Varshneya, 1994).

Soda-lime glass contains about 72% SiO_2, 14% Na_2O, 10% CaO, and 2% Al_2O_3 (Wikipedia, www, 2008). In soda-lime glass, sodium (Na^+) and calcium (Ca^{2+}) ions are inserted into the silicate ion structure such that the tetrahedrons of silicon and oxygen atoms are stretched. The glass transition temperature (T_g) is about 550°C and the melting point is about 1000°C.

Whereas pure SiO_2 glass does not absorb UV light, soda-lime glass does not allow light at a wavelength of shorter than 400 nm (UV light) to pass. The disadvantages of soda-lime glass are that not resistant to high temperatures and sudden thermal changes. For example, everybody has experienced a glass breaking down when pouring liquid at high temperature, e.g. to make tea. Some of the use of soda-lime glass is primarily used for bottles, jars, everyday drinking glasses, and window glass (Lenntech, www, 2009).

2.1.2 Non-Silica-Based Oxide glasses

Oxide glasses that do not have silica as a principal component do not have much commercial use. B_2O_3-based glasses and P_2O_5-based glasses are readily attacked by water. However, their study has been extremely important towards enhancing our understanding of glass structure. About the only non-silica oxide glasses that have some commercial interest are the boroaluminates (e.g. "Cabal" glasses with electrical resistivities exceeding that of silica) (Varshneya, 1994), Alkali oxide borate glasses [x $M_2O \cdot (1-x)$ B_2O_3] are of interest as sealing glasses for electrochemical, electrical, electronic and optical applications. The fusion

temperatures (at which the viscosity value is 20 Pa.s) of these glasses are around 600°C. The viscosity of alkali oxide borate glass melt is very sensitive to the temperature and the composition (Dr. Saad B. H. Farid, 2008), alkaline earth aluminates (as a high-temperature sealant and IR-transmitting glass), and V_2O_5-based glasses. Many glasses, where large amounts of V_2O_5, TeO_2, Bi_2O_3, or Sb_2O_3 are present in addition to some silica, have very low liquidus temperatures. Such glasses can be quite fluid at ordinary temperatures. Hence, some of theses glasses have found use in glass sealing of electronic components. Tellurite glasses are used for optical systems because of their special properties; very high refractive indices (in excess of 2.0) (Varshneya), wide transmission window, good glass stability and durability , high refractive index, large non-linear optical sensibility, relatively low phonon energy in blue (Lee et al., 1991) and green band emission (Kishino et al., 2000) region. The broadband erbium-doped fiber amplifiers have been demonstrated using TeO_2-based glass fibers as host materials (Ohishi et al., 1998).

2.2   Luminescence

The luminescence is the phenomenon in which the materials absorb the energy dand emits VIS or near-VIS light subsequently. The excitation is performed by the irradiation of light or high energy particles, mechanical stresses, chemical reaction and heat treatment. When the emission of light occurs during excitation and within 10^{-8} second, it is called "Fluorescence". Here, the period of 10^{-8} second means that this period is the same as the life time of excited state for allowed transition of electric dipole in VIS region. If the emission continued after excitation, this is called as "Phosphorescence" or "After glow". The solid material which exhibits luminescence is called as "Phosphor".

Luminescence is the emission of optical radiation (infrared, visible, or ultraviolet light) by matter. It represents the conversion of energy from one form to another, in this case, light. This phenomenon is to be distinguished from incandescence, which is the emission of radiation by a substance by virtue of its being at a high temperature (>500°C). Luminescence can occur in a wide variety of substances and under many different circumstances. Thus, atoms, various kinds of molecules, polymers, organic or inorganic crystals, amorphous substances or even biological units can luminance under appropriate conditions. The common aspect to observe luminescence is when an atom or molecule emits a photon (a quantum of light), there is change in its electronic structure.

When electrons are confined to a region of space that is defined by the position of the atomic centers of a molecule (or just the nucleus, in the case of an atom), a set of discrete energy levels is imposed on the system. In the case that some process delivers an appropriate amount of energy to the system, the electronic structure can be changed to an excited state. The release of this extra energy, and thus the way back to the initial state (ground state) can occur via the emission of a photon. Dependent on whether the spin quantum number of the electrons is change in the emission process or not, one may distinguish two different types of luminescence: fluorescence, in which emission occurs with no net change of the spin quantum number, and phosphorescence, in which emission is accompanied by a change in the spin quantum number. These have the consequence that fluorescence is much shorter-lived (ca.10^{-9}-10^{-7} s) as compared with phosphorescence (ca. 10^{-3}-10 s). However, to life apply this rule correctly; the spin state of the system under investigation has to be known in detail, which is, especially for complex systems, rarely the case. Another way to get

some sort of order in the widespread phenomenon of light emission of matter is to distinguish the modes of luminescence production, that is, the way in which the electronic system is excited. Other common types of luminescence and their modes of production are as follows: (Halpern, 2005)

2.2.1 Radioluminescence

Radioluminescence (or scintillation) is produced by ionizing radiation. Some polymers contain organic molecules that emit visible light when exposed to such radiation as x-ray, γ-ray, or cosmic ray, and thus act as detectors for high-energy radiation. Scintillators are organic molecules that emit visible light when they are excited by the decay products of certain radioactive isotopes such as 3H (tritium), 14C, and 18O, and are used in many biomedical applications.

2.2.2 Electroluminescence

Electroluminescence is produced by the exposure of atoms or molecules to an electric field or plasma. An example is the gas-discharge tube. These are lamps that are filled with a gas such as neon, argon, xenon, nitrogen, etc. or the vapor of metals such as mercury or sodium. The lamps contain electrodes, which are connected to an electrical power supply. The applied voltage is high enough to ionize the atoms and produce a low-pressure plasma, or ionic (current-carrying) gas. The recombination of metal ions and electrons in the plasma leads to the production of electronically excited states of the atoms and hence the emissions of light, usually in the form of very narrow lines throughout the electromagnetic spectrum. The common fluorescence lamp is a discharge tube in which electronically excited mercury atoms transfer this energy to a material called a phosphor, which are coated the inside surface of the tube. The phosphor, after being excited by collisions with electrons or

light produced by atoms or molecules, emits most of the observed light. Another example is lightning, in which the static electricity generated by a moving air mass ionizes (removes electrons from) the nitrogen and oxygen molecules. Charge recombination produces nitrogen molecules in an excited electronic state, which release this energy by emitting radiation as visible light. The Northern Lights (aurora borealis) also represents an example of this type of luminescence. Electroluminescence is produced by the familiar light-emitting diode, which is constructed from a pair of aluminum-gallium-arsenide (AlGaAs) sheets in contact with each other. One contains impurities that add electrons, while the other has deficiencies of electrons. When an electric current flows between the sheets, electrons are promoted to a higher energy level (the conduction band), and the subsequent of these electrons to a lower level (the charge-depleted sites) result in the emission of light, often in the red region of the spectrum.

2.2.3 Chemiluminescence

Chemiluminescence is produced as a result of a chemical reaction usually involving an oxidation-reduction process, in which, simply viewed, electronic charge is transferred from one species to another with the resultant formation of an excites state. One common example is the luminol reaction. When luminol, an aminosubstituted phthalazine derivative, is treated with base and an oxidizing agent such as hydrogen peroxide, nitrogen molecules are produced along with the emission of blue light. This light comes from the excited state of a product, the aminophthalate molecule. In this example, the light emitted represents the conversion of chemical energy to optical energy.

2.2.4 Bioluminescence

Bioluminescence is the result of certain oxidation processes (usually enzyme-catalyzed) in biological systems. The firefly and its larva, the glowworm, are well-studied examples: light emission for the firefly serves as a mating signal. These organisms produce a molecule called luciferin and an enzyme known as luciferase. When these molecules are in the presence of oxygen and adenosine phosphate, yellow-green light is produced with very high efficiency. Many other organisms such as bacteria, fungi, and certain marine species are bioluminescent. It is thought that chemiluminescence is a now-defunct evolutionary mechanism that was developed by some anaerobic organisms for the disposal of oxygen, which can be toxic to organisms.

2.2.5 Thermoluminescence (TL)

Thermoluminescence (TL) is light produced when a substance, previously exposed to ionizing radiation, is heated. Many natural substances, such as quartz and feldspar, are exposed to ionizing radiation produced by radioactive decay of the isotopes of elements such as potassium, thorium and uranium that are present in their immediate environment (and also from cosmic rays). As a result of this exposure, electrical charges are gradually placed in low-energy sites in the solid called traps. When this substance is heated, these (opposite) charges recombine; producing luminescence whose intensity reflects the number of stored-up charges. If in some past event the material became heated, either through geological processes or anthropological activities, the accumulated charge pairs are depleted (the "clock is reset"), and their population again increases with time. Deliberate exposure of the sample to heat at some later time produces TL, which can be used to date it. Alternatively, this light can be released by exposing the sample to light in a technique called Optically Stimulated Luminescence.

2.2.6 Triboluminescence

Triboluminescence is light emitted when a solid is subjected to friction, such as when it is scratched, ground, or rubbed. The luminescence produced by some minerals in this way is akin to thermoluminescence, except that a mechanical stimulus, rather than bulk heating, causes the effect. In other cases involving organic solids, such as sucrose, the frictional forces result in charge separation, which, in turn, leads to the production of electronically excited nitrogen molecules that emit light (similar to what is seen in lightning). Crushing candy products that contain wintergreen flavor (salicylate), causes a bright blue triboluminescent response. In this case the excited nitrogen (or other species) transfers its energy to the salicylate it to fluoresce. Although there is a wide range of circumstances in which luminescence is observed, there is one common to this phenomenon. For solid state materials charge recombination produces the excited state of the emitting species. In the case of atoms or molecules, luminescence results from the transition between discrete energy levels. The luminescence is due to the addition of a luminogen or activator in the form of a trace impurity, for example, in phosphorescent sulphides, copper, manganese, bismuth. In some cases crystal lattice defects provide localized levels, like those of impurity, which play the part of the activator. Stimulated emission (laser action) requires an inverted ion population of the excited species and has been achieved for a large number of ions and transitions at wavelengths ranging from the far infrared to soft x-ray. Solid-state lasers incorporate many different transition-metal ions, organic dyes, and color center in inorganic and organic crystalline and amorphous hosts. Lasing is produced principally by optical pumping. In semiconductor-junction laser materials, a large electron current creates excited electron and hole states and induces laser action.

2.3   Redox Equilibrium in glasses

Oxidation is the loss of an electron and reduction is the reverse:

$$Fe^{3+} + electron \xrightarrow{\text{reduction}} Fe^{2+} \qquad (2.1)$$

The simultaneous occurrence of oxidation and reduction is commonly known as a "redox process". When a metal, M forms an oxide MO_x, it can be visualized that the metal electrons are transferred to the empty 2p orbitals of the oxygen atom and thus the elementary steps of the reaction can be hypothetically written as:

$$M \longrightarrow M^{2+} + electrons \ (oxidation) \qquad (2.2)$$

$$xO + 2x \ electrons \longrightarrow xO^{2-} \ (reduction) \qquad (2.3)$$
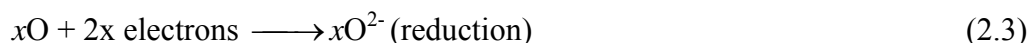
The redox reaction in glass melt may be written in different ways, for example the redox reaction of ferrous and ferric iron, the reaction may be written in terms of the pure oxide as:

$$4FeO \ (glass) + O_2 \ (glass) \longleftrightarrow 2Fe_2O_3 \ (glass) \qquad (2.4)$$
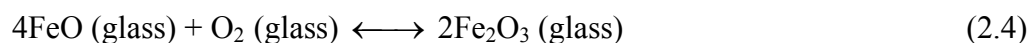
$$K = [\alpha_{(Fe_2O_3)}]^2 / [\alpha_{(FeO)}]^4 \cdot [p_{(O_2)}] \qquad (2.5)$$

where K is the redox equilibrium constant, a is the activity of oxide in glass, pO_2 is partial pressure of oxygen.

The redox reaction may also be written in terms of the ionic species present in the system as:

$$4Fe^{2+} \text{ (glass)} + O_2 \text{ (glass)} \longleftrightarrow 4Fe^{3+} \text{ (glass)} + 2O^{2-} \text{ (glass)} \qquad (2.6)$$
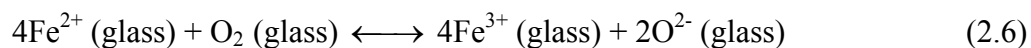
When a redox oxide is introduced into a glass melt, it distributes itself into different states of oxidation depending upon the time and temperature of melting, the glass composition, the furnace atmosphere and batch composition.

2.3.1 Effect of melting temperature on the redox equilibrium in glasses

The oxidation-reduction equilibrium in glass usually moves toward the reduced side with increasing temperature. This can be explained by using standard thermodynamic data. The redox equilibrium constant, K, is related to the temperature of reaction by the Van't Hoff isochore:

$$\frac{d \ln K}{dT} = \frac{\Delta H}{RT^2} \qquad (2.7)$$

where ΔH is the enthalpy, R is the gas constant and T is the absolute temperature. On integration

$$\ln K = -\frac{\Delta H}{RT} + I \qquad (2.8)$$

where I is the integration constant.

From the above equation, the plot of the ratio: log [(concentration of oxidized form)/(concentration of the reduce form)] against reciprocal of absolute temperature (1/T) should give a straight line, with slope equivalent to $-\Delta H/(R \times 2.303)$. The slope of the lines is positive, indicating that these reactions are exothermic and that they will proceed towards the reduced side at higher temperature.

2.3.2 Effect of glass composition on the redox equilibrium in glasses

All experiments on redox equilibria reported that the proportion of the redox ion in the higher oxidation state increases with the basicity. Comparing these results with equation (6) for the redox equilibrium in glasses, the conclusion must be that oxygen ion activity decreases with increasing basicity. This apparent paradox is resolved by recognizing that the concentration equilibrium constant K, which was measured in these cases, varies with composition. Further, transition metal ions occur as different complexes in glass, and not free ions as written in Eq. (6). When redox equilibria are written in terms of these complexes, instead of free ions, a satisfactory qualitative correlation may be obtained between the oxygen ion activity and the redox equilibrium. Finally, the more basic the alkali oxide and the greater its concentration, the more redox reaction (Eq.6) will move to the right side and higher valence state will be formed.

The basicity of glasses can be evaluated according to Duffy's optical basicity scheme (Duffy, 1996).

2.3.3 Effect of additives on the redox equilibrium in glasses

In the glass melting, the main ingredients of soda-lime silicate glasses are sand, sodium carbonate, limestone, dolomite, and minerals containing alumina. In addition to melting aids such as borates and fluorspar there are two other groups of supplementary raw materials in use; those which have a reducing effect and those which are oxidizing. Carbon and calumite slag are widely used as reducing agents and sulfate and nitrate of alkaline metal for oxidizing agent.

2.4   Color center in glasses

It is well known that color generation of glasses in visible (VIS) region is basically caused by impurities, such as transition metal ions, rare earth ions, nano-scale metal and semiconductors particles, etc. (Sigel, 1977). The mechanism of coloration of transition metal ions and rare earth ion has been recognized almost completely based on "Ligand field theory" (Kamimura, Sugano, and Tanabe, 2005; Bates, 1994), and their energy levels could be calculated. The coloration of metal and semiconductors particles have also been understood based on "Surface plasmon resonance theory" and "Band gap coloration" (Varshneya, 1994). The brilliant gold ruby-red glasses and yellow-red CdS_xSe_{1-x} containing glasses are included in this group. It is believed that the nano-scale Au particle (Hayakawa, Fukunaga, Tai, Murakami, and Nakamura, 2006; Vreugdenlik, Pilatzke, and Parnis, 2006) and CdS particles (Chen, Wang, and Lin, 1977; Miyoshi, Towata, Matsuki, and Matsuo, 1997) are present in these glasses.

There are numerous other sources of VIS coloration in glasses which are of interest. Included in this group are blue-sulfur, pink-selenium, and purple-green tellurium whose colors are associated with elemental clustering (Sigel, 1977). The word of "cluster" is used as the aggregation of elements or atoms, (M)n, here n is normally smaller than 1,000,000. In these glasses, non-metal elements of sulfur, selenium and tellurium are present as the form of molecular ions, such as S_2^-, S_3^- (Ahmed et al., 1997), Se_2, Se_2^- (Paul, 1975; Guha et al., 1998) and Te_2, Te_2^- (Lindner et al., 1996; Konishi et al., 2003), respectively. The energy levels of these species have been discussed based on molecular orbital theory, and the luminescence characteristics of these species have also discussed.

Ahmed et al. (1997) investigated Raman spectra of sodium and potassium borate glasses (20-30 mol% Na_2O and 5-35 mol% K_2O) doped with sulfur in various concentrations (0.3-6 wt%) and melted at $1000\pm10°C$ for 2 h. The glasses were annealed at 300-350°C for 30 min depending on alkali content. From UV-VIS absorption and Raman spectra, they found that Se_3^- and Se_2^- is definitely formed in blue glasses of 15-30 mol% K_2O containing borate glasses and 20-35 mol% Na_2O and K_2O, respectively

Guha et al. (1998) studied and identified Se_2^- centers in Se-doped potassium borosilicate glasses by ESR, Raman, UV-VIS absorption and PL spectroscopy. The glass sample was prepared by melting at 1300°C for 2 h. The ESR spectra of all sample show a lineshape that is attributed to orthorhombic symmetry around the molecule. PL spectra show a broad luminescence band between 500 and 900 nm which is identified as $^2\Pi_u \rightarrow {}^2\Pi_g$ transition of Se_2^-. An electron-lattice interaction gives rise to overtones of fundamental vibration (322 cm^{-1}) of Se_2^- molecule and they are identified by Raman scattering measurements.

Lindner et al. (1996) reported the synthesis and spectroscopic properties of blue and green tellurium ultramarines, both possessing sodalite-type structures. From Raman spectroscopy they found that the color is generated by Te_2 as well as Te_2^- species, in the case of hydrothermally synthesized greenish tellurium-doped sodalite, the same ditellurium species are identified by means of UV-VIS, luminescence and Raman investigations

Konishi et al. (2003) investigated glass formation and color properties in the P_2O_5-TeO_2-ZnO system of glass. Glasses were melted at 900, 1000, 1100 and 1200°C. They found that the color of samples varied from clear to deep red depending on the

composition and melting temperature, and the color became deeper with increasing TeO_2 content and melting temperature. From results of SEM and XPS analyses, they concluded that the red coloration is due to colloidal metallic Te.

Khonthon, S., et al. (2007) investigated the color center and luminescence characteristic of Te-doped glasses and glasses-ceramics, and they have found that the NIR luminescence centered at 1250 nm with a half width of 250 nm in Te-doped glasses and glasses ceramic (0.2 wt%Te-Sp, 1.6 wt%Te-SL, 14.07 wt%Te-ZTP system of glass and melting at 1600, 1450 and 1200°C, respectively) which are discovered for the first time. They concluded that the coloration and NIR luminescence might be due to the elemental clustering such as Te_2/ Te_2^- by ESR.

CHAPTER III

EXPERIMENTAL

3.1   Starting materials

Raw materials used in this research are listed in Table 3.1

Table 3.1 Raw materials used in this research.

Raw materials	Chemical formula	Make	Remarks
Silica sand	SiO_2	Rayong sand, Thailand	-
Silica	SiO_2	Kojundo Chemicals	99.90%
Alumina	Al_2O_3	Sumitomo Chemicals Ind.	A-21
Sodium carbonate	Na_2CO_3	Carlo Erba	Reagent grade chemical
Potassium carbonate	K_2CO_3	Carlo Erba	"
Calcium carbonate	$CaCO_3$	Carlo Erba	"
Magnesium carbonate, basic	$3MgCO_3.$	Riedel-de Haen	"
	$Mg(OH)_2.3H_2O$		MgO: 40%
Zinc oxide	ZnO	Carlo Erba	"
Boric acid	H_3BO_3	UNIVAR	"
Tellurium oxide	TeO_2	Fluka	"
Activated carbon	C	Fluka	"

3.2 Sample preparation

3.2.1 Effect of melting temperature : Te-containing borate glasses

The glass composition used was $63B_2O_3 \cdot 9Al_2O_3 \cdot 9ZnO \cdot 9K_2O \cdot 10TeO_2$ (mol%). Reagent grade chemicals of H_3BO_3, Al_2O_3, ZnO, K_2CO_3 and TeO_2 were used as raw materials. Batches corresponding to 25 g of glass were mixed thoroughly and melted in 50 cc alumina crucible under various conditions (850-1300°C for 15-60 min) in an electric furnace in air. The melting conditions of glasses are shown in Table 3.2. After melting they were poured onto iron plate and pressed by another iron plate. Then they were annealed at 450°C for 30 min and cooled slowly to room temperature in the furnace. All glasses were polished optically into about 1.5-2.0 mm in thickness for optical measurement. Hereafter, these glasses are referred to as Te-850, Te-1000, Te-1100, Te-1200 and Te-1300, respectively.

Table 3.2 Melting conditions of glasses

Glass No.	Melting conditions (°C–min.)
Te-850	850-60
Te-1000	1000-20
Te-1100	1100-20
Te-1200	1200-20
Te-1300	1300-15

3.2.2 Effect of glass composition : Te-containing borate glasses

The compositions of glasses used are $90[(80-X) B_2O_3 \cdot 10Al_2O_3 \cdot 10ZnO \cdot XK_2O] \cdot 10TeO_2$ (mol%, X=0, 10, 20 and 30). Reagent grade chemicals of H_3BO_3, Al_2O_3, ZnO, K_2CO_3 and TeO_2 were used as raw materials. Batches corresponding to 25 g of glass were mixed thoroughly and melted in 50 cc alumina crucible at 1200°C for 20 min in an electric furnace in air. After melting they were poured onto iron plate and pressed by another iron plate. Then they were annealed at 450°C for 30 min and cooled slowly to room temperature in the furnace. All glasses were polished optically into about 1.5-2.0 mm in thickness for optical measurement. Hereafter, these glasses are referred to as X=0, X=10, X=20 and X=30, respectively.

3.2.3 Effect of carbon addition (reducing agent) : Te-containing
borate glasses

The glasses of $63B_2O_3 \cdot 9Al_2O_3 \cdot 9ZnO \cdot 9K_2O \cdot 10TeO_2$ (mol%) were prepared by adding 0, 0.24, 0.5 and 1.0 wt% of carbon. In order to control the melting atmosphere, carbon was added to batches. Reagent grade chemicals of H_3BO_3, Al_2O_3, ZnO, K_2CO_3, TeO_2 and activated carbon were used as raw materials. Batches corresponding to 25 g of glass were mixed thoroughly and melted in 50 cc alumina crucible at 1000°C for 30 min in an electric furnace in air. After melting they were poured onto iron plate and pressed by another iron plate. Then they were annealed at 450°C for 30 min and cooled slowly to room temperature in the furnace. All glasses were polished optically into about 1.5-2.0 mm in thickness for optical measurement. Hereafter, these glasses are referred to as C-0, C-0.24, C-0.5 and C-1.0, respectively.

3.2.4 Effect of carbon addition (reducing agent) : Te-doped soda-lime-silicate glasses

The glasses of $72SiO_2 \cdot 2Al_2O_3 \cdot 4MgO \cdot 8CaO \cdot 13Na_2O \cdot 1K_2O \cdot 1TeO_2$ $\cdot Xcarbon$ (wt%, X=0, 0.1, 0.2, 0.3, 0.5 and 1.0) were prepared. In order to control the melting atmosphere, carbon was added to batches.

High purity silica sand, alumina and reagent grade chemicals of MgO, $CaCO_3$, Na_2CO_3, K_2CO_3, TeO_2 and activated carbon were used as raw materials. Batches corresponding to 25 g of glass were mixed thoroughly and melted in 50 cc alumina crucible at 1450°C for 1 h in an electric furnace in air. After melting they were poured onto iron plate and pressed by another iron plate. Then they were annealed at 600°C for 30 min and cooled slowly in the furnace. The glasses were cut and polished optically into about 1.5-2.0 mm in thickness for optical measurements. Hereafter, these glasses are referred to as C-0, C-0.1, C-0.2, C-0.3, C-0.5 and C-1.0, respectively.

3.2.5 Effect of TeO_2 concentration : Te-doped soda-lime-silicate glasses

The glass compositions used were $72SiO_2 \cdot 2Al_2O_3 \cdot 4MgO \cdot 8CaO \cdot 13Na_2O$ $\cdot 1K_2O \cdot XTeO_2 \cdot 0.3carbon$ (wt%, X= 0.2, 0.5, 0.7, 1.0 and 2.0). High purity silica sand, alumina and reagent grade chemicals of MgO, $CaCO_3$, Na_2CO_3, K_2CO_3, TeO_2 and carbon were used as raw materials. Batches corresponding to 25 g of glass were mixed thoroughly and melted in 50 cc alumina crucible at 1450°C for 1 h in an electric furnace in air. After melting they were poured onto iron plate and pressed by another iron plate. Then they were annealed at 600°C for 30 min and cooled slowly in the furnace.

The glasses were cut and polished optically into about 1.5-2.0 mm in thickness for optical measurements. Hereafter, these glasses are referred to as Te-0.2, Te-0.5, Te-0.7, Te-1.0 and Te-2.0, respectively.

3.2.6 Structure and properties of TeO_2- containing borate glasses

TeO_2- containing borate glasses of $(100-X)[80B_2O_3 \cdot 10Al_2O_3 \cdot 10ZnO]$ $\cdot XTeO_2$ (mol%, X=0, 10, 20 and 30) were prepared by conventional melt-quench method. High purity alumina and reagent grade chemicals of H_3BO_3, ZnO, TeO_2 were used as raw materials. Batches corresponding to 30 g of glass were mixed thoroughly and melted in 50 cc alumina crucible at 1000–1200°C for 30 min depending on the glass composition in an electric furnace in air. After melting they were poured on to iron plate and pressed by another one. Then they were annealed at 400°–500°C for 30 min depending on the glass composition in the furnace, and cooled to room temperature in the furnace.

Some glasses were cut into about $0.5 \times (2.5\text{-}3.0) \times 0.3$ cm^3 for the measurement of glasses transition point (Tg) expansion coefficient (α) using fused silica single push rod type dilatometer (Netsch 402E) and all glasses were pulverized into #200 pass for DTA and X-ray absorption measurement. Hereafter, these glasses are referred to as Te-0, Te-10, Te-20, Te-30, respectively.

3.3　Characterization

3.3.1　X-ray Diffraction (XRD) analysis

Crystalline phases were examined by powder X-ray diffraction (XRD) using Bruker AXS Model D5005 under the condition of Cu-Kα radiation at 40 kV and 40 mA., slit system; 1°-1°, scan; step scan 0.02°/step, scan speed 100 sec./step (very slow scan).

3.3.2　Thermal analysis : Differential thermal analysis (DTA)
and Dilatometer

The differential thermal analysis (DTA) was carried out routinely using SDT 2960 Simultaneous Differential Thermal Analyzer (STA) in TGA-DTA mode at the heating rate of 10°C/min.

Glass transition temperature (Tg), dilatometric softening point (Td) and thermal expansion coefficient (α) were measured for some glasses using fused silica single push rod type dilatometer (Netsch 402E) at the heating rate of 5°C/min.

3.3.3　Scanning Electron Microscopy (SEM) Analysis

The surface structures of glasses were observed by scanning electron microscope (SEM) using JEOL, JSM 6400. The fractured surface of glasses were etched by 0.5%HF solution for 1 min at room temperature and coated with conductive material (Au) by using Ion Sputtering Device (JEOL, JFC-110E).

3.3.4　Electron Spin Resonance (ESR) Analysis

The electron spin resonance spectra were measured using JEOL JES RE-2X at room temperature. Microwave unit: X band, frequency: 8.8-9.6 GHz, cavity: cylindrical, operating in TE_{011} mode and ESR software: use ES-IPRIT program.

3.3.5 Optical Analysis

The absorption spectra were measured with using Cary 1E ultraviolet-visible (UV-VIS) spectrometer in the range of 300-800 nm at room temperature.

The NIR luminescence spectra were measured under the excitation of 974 nm laser diode in the range of 1000-1700 nm at room temperature. The optical setup for NIR luminescence measurement is shown in Figure 3.1. Emission from the samples was dispersed by a single monochromator (blaze, 1.0 mm; grating, 600 grooves/mm; resolution 3 nm) and detected by InGaAs photodiode.
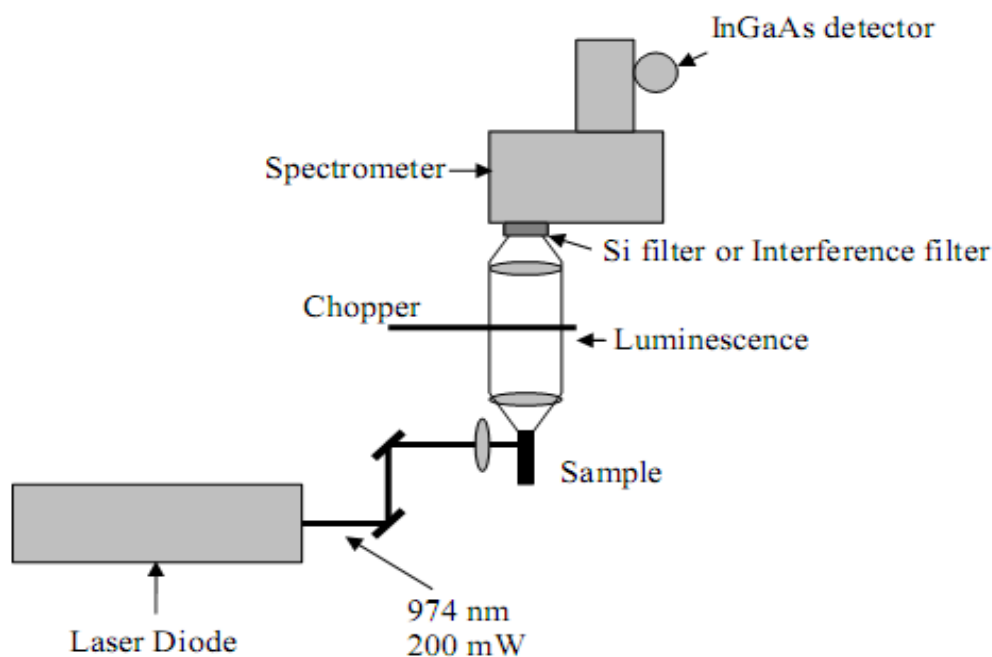
Figure 3.1 The optical setup for NIR luminescence measurement.

3.3.6 X-ray Photoelectron Spectroscopy (XPS) Analysis

The X-ray Photoelectron Spectroscopy (XPS) measurement was performed with monochromatized Mg-Kα radiation at acceleration voltage of 15 kV with electron shower for Te $3d_{5/2}$ and $3d_{3/2}$ (Synchrotron Light Research Institute, Thailand). The shift of the energy scale was corrected with a reference of C1s binding energy of residual hydrocarbon at 284.6 eV.

3.3.7 X-ray absorption spectroscopy (XAS) Analysis

Te L_{III} (4341 eV) edge X-ray absorption near edge structure (XANES) spectra were obtained on BL-8 beam line at Synchrotron Light Research Institute, Thailand. The primary beam was obtained by a double crystal Si (111) monochromator. The energy steps and scan time were 0.2 eV/step and 5 times, respectively. The Fluorescent-mode was applied. The reagent grade chemical of α–TeO_2 (para-tellurite) was used as a standard. The research procedure is shown in Figure 3.2.

Batch Preparation	► High purity silica sand, alumina
	► reagent grade chemicals of;
	- MgO - $CaCO_3$
	- Na_2CO_3 - K_2CO_3
	- H_3BO_3 - ZnO
	- TeO_2 - Carbon

Mixing
15-20 min

| Melting
Alumina Crucible | Borate glasses; 850-1300°C, 15-60 min

Soda-lime-silicate glass; 1450°C, 60 |

Casting
Iron plate

| Annealing | Borate glasses; 450°C, 30 min

Soda-lime silicate glass; 600°C, 30 min |

Sample Preparation
1. Plate for optical and thermal properties measurement by
   cutting & polishing (SiC, CeO_2 powder) into about $2\times2\times(0.1$-$0.3)$
   cm^3 and $0.5 \times(2.5$-$3.0)\times 0.3\ cm^3$ respectively.
2. Powder samples
   Pulverizing (<200#)

Characterization

Figure 3.2 Flow chart of experimental procedure.

```
┌─────────────────────┐
│ Sample Preparation  │
└─────────────────────┘
```

Characterization (Plate Sample)

- UV-VIS-NIR Spectrometer: Absorption spectra

- Specified NIR Photoluminescence Spectrometer:

  Photoluminescence spectra in NIR region

- X-ray Photoemission Spectroscopy (XPS): Determination

  of valence state

- Dilatometer: Measurement of glass transition point (Tg)

  and thermal expansion coefficient (α)

Characterization (Powder Sample)

- Electron Spin Resonance (ESR) spectra : Detection of

  color center and luminescent center

- X-ray Absorption Near Edge Structure Spectroscopy

  (XANES): Determination structure of TeO_2

- Simultaneous Differential Thermal Analyzer (STA):

  Measurement of glass transition temperature (Tg)

```
┌─────────────────┐
│ Data Analysis   │
└─────────────────┘
```

Figure 3.2 Flow chart of experimental procedure (Cont.).

CHAPTER IV

RESULTS AND DISCUSSION

4.1 Effect of melting temperature : Te-containing borate glasses

4.1.1 Results

4.1.1.1 Appearance and absorption spectra

The colors of glasses change from colorless (Te-850) to reddish brown (Te-1300) with increase in melting temperature. Appearances and absorption bands of these glasses are summarized in Table 4.1.

Table 4.1 Appearances and absorption bands analyzed by Gaussian distribution.

Glass No.	Appearance	Absorption bands/nm			
		I	II	III	IV
Te-850	Colorless	–	–	–	–
Te-1000	Pale orange	335**	443	535*	–
Te-1100	Orange brown	343**	445	524*	–
Te-1200	Reddish orange	356	431**	523	–
Te-1300	Reddish brown	354	424**	514	–
ZTP*	Brilliant purple	375	417	537	600
Te-SL*	Pale green	374	444	526**	625
Te-Spinel*	Brownish pink	–	420 488**	556	599

Remarks: * Khonthon, S., et al. (2007), ** very weak

Figure 4.1 shows absorption spectra of glasses. In Figure 4.2 the absorption spectra were analyzed and separated into three bands using peak fitting with Gaussian distribution, a sum of three Gaussian spectral functions are shown three absorption bands at 18709 cm^{-1} (535 nm), 22566 cm^{-1} (443 nm) and 29865 cm^{-1} (335 nm) for Te-1000 glass and 19096 cm^{-1} (524 nm), 22469 cm^{-1} (445 nm) and 29148 cm^{-1} (343 nm) for Te-1100 glass. The results are shown in Table 4.1.
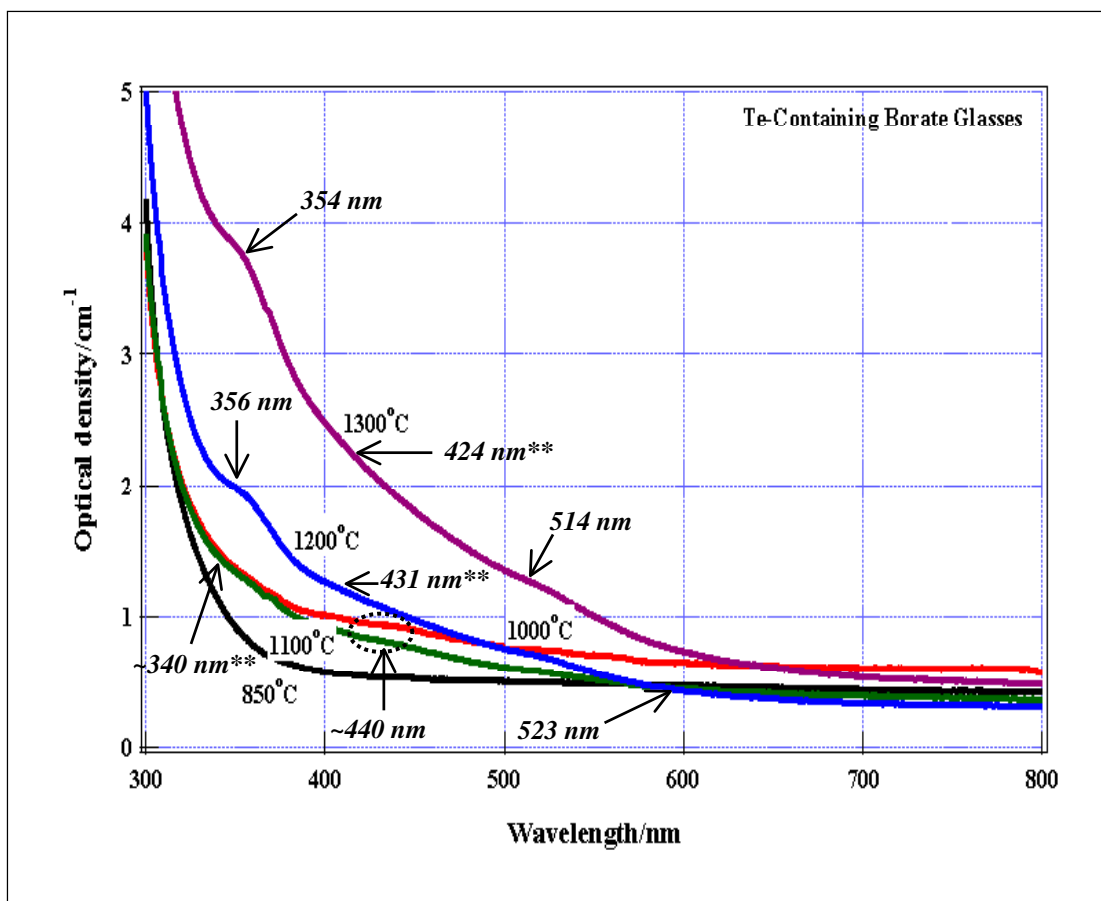
Figure 4.1 Absorption spectra of Te-containing borate glasses.
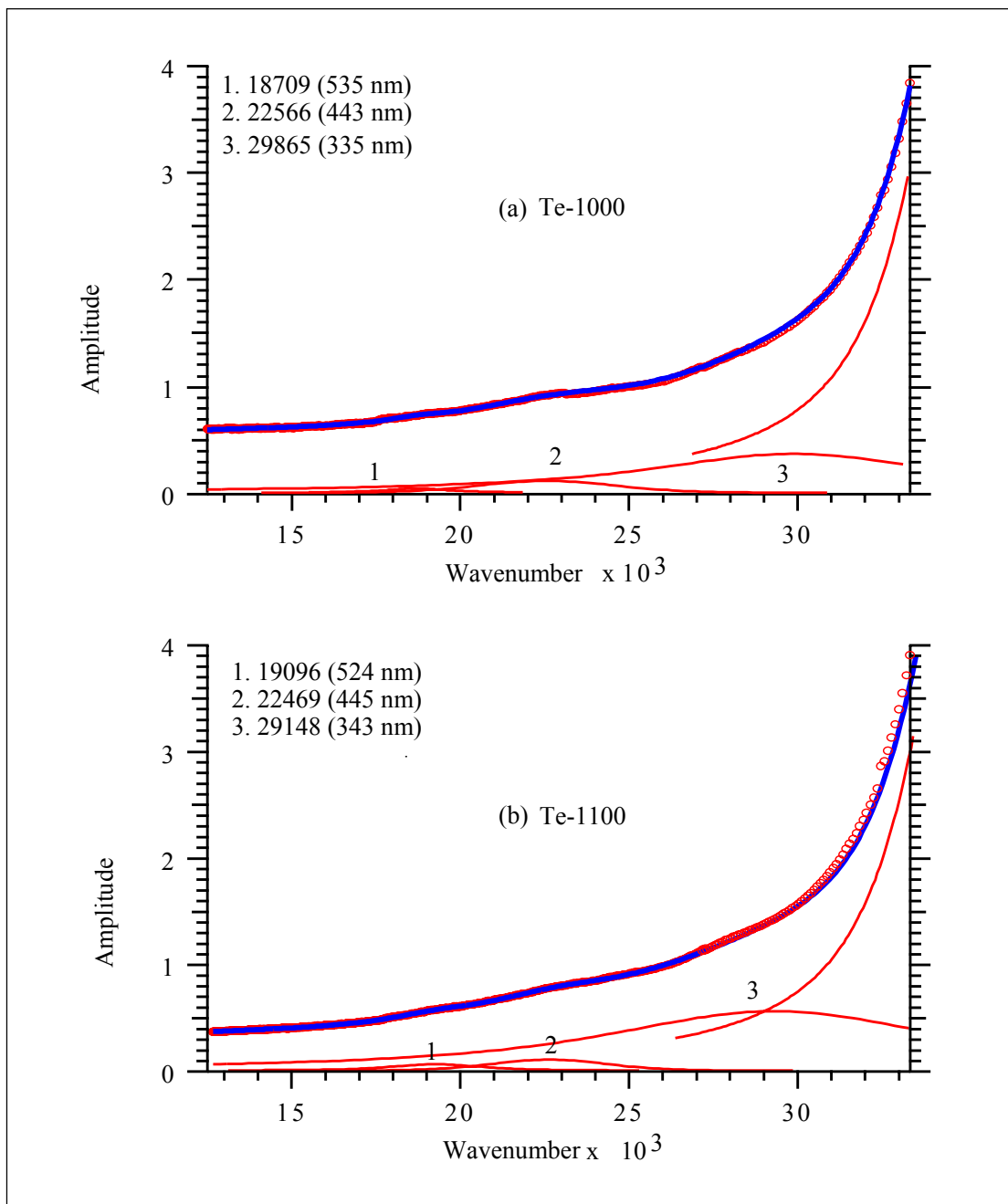
Figure 4.2 Experimental absorption spectra (as seen in Figure 4.1) are further

shown here as a sum of three Gaussian spectral functions

of (a) Te-1000 and (b) Te-1100 glasses.

No characteristic absorption bands in ultra-violet (UV) to visible region can be observed for Te-850 glass. Basically, three absorption bands can be observed, ~370 nm (Band I), ~430 nm (Band II) and ~530 nm (Band III), respectively. The assignment of these absorption bands are already known that Band I is exciton transition. Band II, the absorption band at 430 nm is ascribed to $^3\Sigma g^-\rightarrow^3\Sigma u^-$ transition of Te_2 color center (Lindner et al., 1996). The assignment of these absorption bands are shown that electrons from tellurium are used to bond in a sigma anti bonding orbital of ground triplet states-to-another state or ligand and result in a charge transfer transition of tellurium and Band III can be assigned to Te metallic colloids (Konishi et al., 2003).

However, these spectral patterns are different from those reported previously (Khonthon et al., 2007). The former three absorption bands are the same, but Band IV at around 600 nm can not be detected in all borate glasses. The assignment of Band IV has already been done and is ascribed to $^2\Pi g\rightarrow^2\Pi u$ transition of Te_2^- (Lindner et al., 1996) . The assignment of these absorption bands are shown that electrons from tellurium are used to bond to the ligand which electrons move from an atomic orbital on another atom or ligand, in the process relieving tellurium of excess negative charge. It is considered that the color center of Te_2^- may be lacking in all borate glasses and different color center is present in these glasses.

4.1.1.2 Near Infrared (NIR) luminescence

No NIR luminescence can be detected in all borate glasses under the excitation of 974 nm laser diode at room temperature.

4.1.1.3 ESR spectra

In order to determine the luminescent center of Te- doped glasses, the ESR spectra were measured. The ESR spectra are shown in Figure 4.3. Two ESR signals were detected at around $g \approx 4.3$ and $g \approx 2.0$ in all glasses. The intensity of ESR signals at $g \approx 4.3$ decreased with increasing melting temperature. This signal is believed to be from impurities, such as Fe^{3+} ion in the sample (Elvers and Weissmann, 2001) and signal at $g \approx 2.0$ due to electron trapped clusters of Te, such as Te_2^-, the NIR luminescent intensity seems to be proportional to the intensity of $g \approx 2.0$ signals of ESR spectra (Khonthon et al., 2007). The similar ESR spectrum was obtained in Se-doped borosilicate glass and it is believed to be due to Se_2^- ions (Guha, Leppert, and Risbud, 1998). In this work, the intensity of the ESR signal at $g \approx 2.0$ reached the maximum at Te-1200 and decreased again with increase in melting temperature. However, the NIR luminescent intensity seems to be not proportion to the intensity of $g \approx 2.0$ signals of ESR spectra.
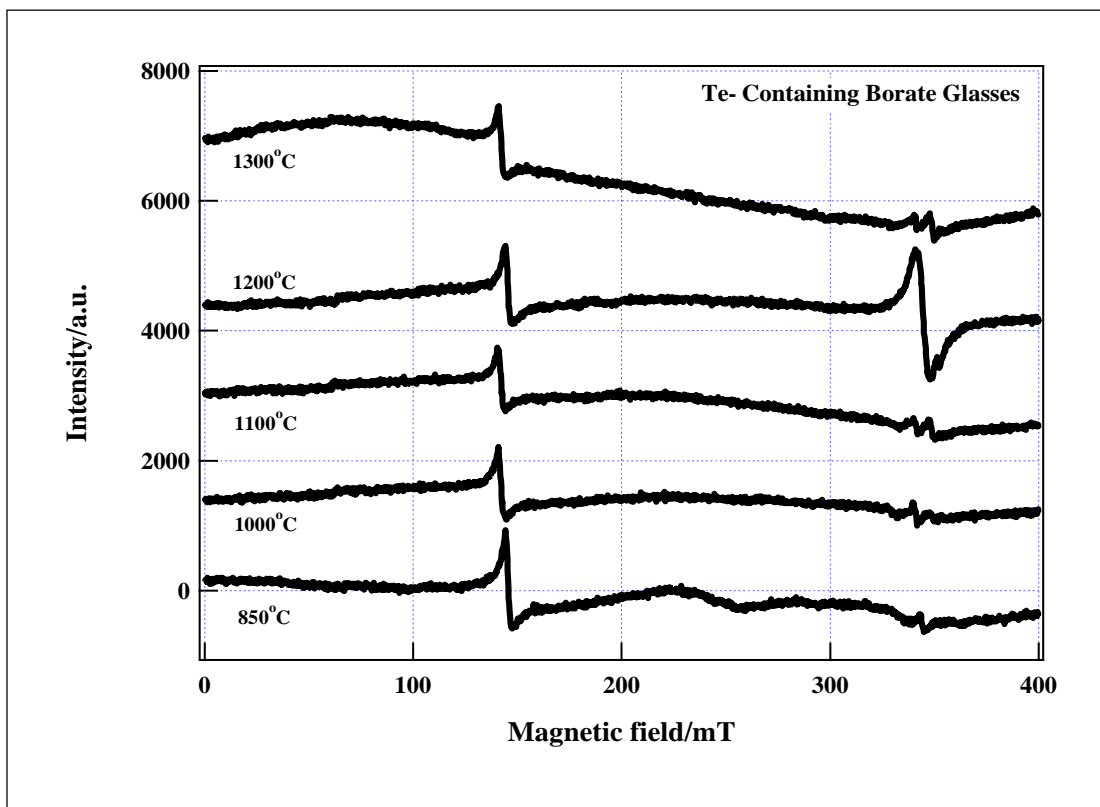
Figure 4.3 ESR spectra of Te-containing borate glasses.

4.1.1.4 XPS spectra

Figure 4.4 displays the Te 3d spin-orbit core level spectra for all glass samples investigated. Two peaks of Te $3d_{5/2}$ and Te $3d_{3/2}$ were detected in all glasses. However, any signal can not be observed in lower energy side of these peaks. From the figure, trend of the peak intensity decreases with increasing melting temperature while the peak positions has not really changed for all temperatures. The binding energies (BE) of the Te $3d_{5/2}$ are measured to be ~ 576 eV as shown in Table 4.2. Full-width at half-maximum (FWHM) increases slightly with increase in melting temperature (2.1±0.3). These values compare very favorable to those obtained on TeO_2 powder-576.1 eV and 2.1 eV for the BE and FWHM, respectively (Mekki et al.,

2006). This indicates that the considerable amount of lower valence species (Te, Te_2, Te_2^-, $(Te)n$ and Te^{2-}) is not present in these glasses.
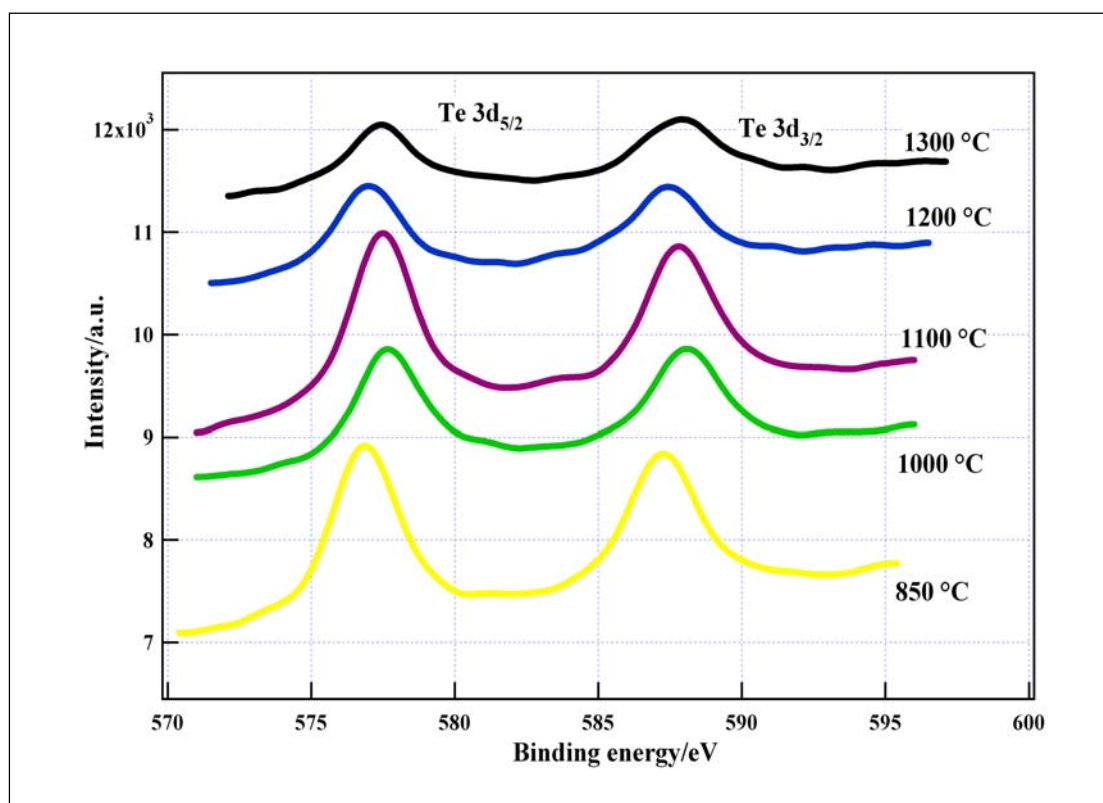
Figure 4.4 Core level Te3d spectra of Te-containing borate glasses.

Table 4.2 Peak positions in eV for the core levels Te $3d_{5/2}$ and their corresponding FWHM (full-width at half-maximum) at different melting temperature of Te-containing borate glasses.

Melting Temperature/°C	Te $3d_{5/2}$/eV	FWHM/eV
850°C	576.7	2.1
1000°C	577.4	1.8
1100°C	577.2	2.1
1200°C	576.7	2.1
1300°C	577.6	2.4

4.2   Effect of glass composition : Te-containing borate glasses

4.2.1 Results

4.2.1.1 Appearance and absorption spectra

The color changes from reddish orange (X=10) to colorless (X=30) with increase in X (increasing amount of K_2O). However, X=0 glass revealed phase separation during casting. Appearances and absorption bands of these glasses are also summarized in Table 4.3.

Table 4.3 Appearance and absorption bands analyzed by Gaussian distribution.

Glass No.	Appearance	Absorption bands/nm			
		I	I	III	IV
X=0	Phase separation	–	–	–	–
X=10	Reddish orange	370	430**	530**	–
X=20	Pale orange	377	430**	530**	–
X=30	Colorless	–	–	–	–
ZTP*	Brilliant purple	375	417	537	600
Te-SL*	Pale green	374	444	526**	625
Te-Spinel*	Brownish pink	–	420 488**	556	599

Remarks: * Khonthon, S., et al. (2007), ** very weak

Figure 4.5 shows absorption spectra of glasses. The absorption spectra were analyzed and separated into three bands using peak fitting with Gaussian distribution. The spectral pattern of these glasses is similar to glasses in previous section (Section 4.1). Three absorption bands can be observed at around 370 nm, 430 nm and 530 nm in X=10 and X=20 glasses. The spectral patterns of both glasses are similar to those of Te-1000~Te-1300 glasses in previous section.

4.2.1.2 Near Infrared (NIR) luminescence

No NIR luminescence can be detected in all borate glasses under the excitation of 974 nm laser diode at room temperature.
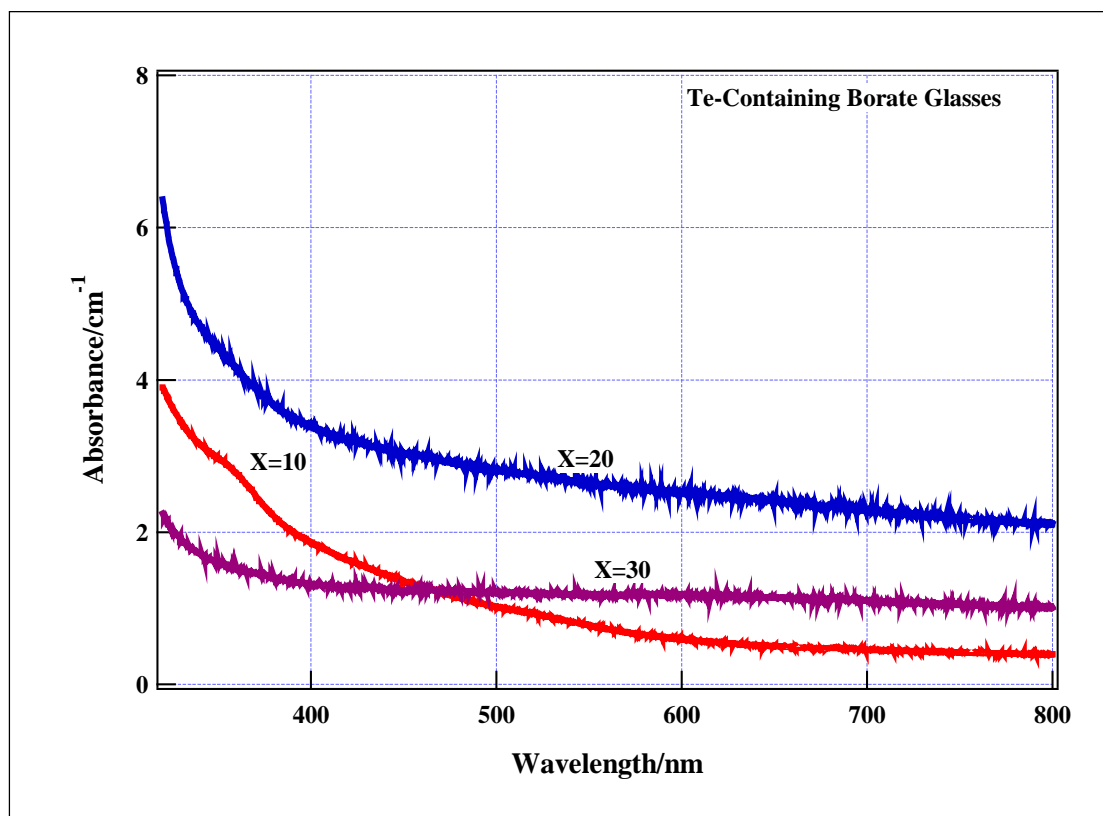
Figure 4.5 Absorption spectra of Te-containing borate glasses.

4.2.1.3 ESR spectra

In order to determine the luminescent center of Te- doped glasses, the ESR spectra were measured. The ESR spectra were measured. The ESR spectra are shown in Figure 4.6. Two ESR signals were detected at around $g \approx 4.3$ and $g \approx 2.0$ in all glasses. The ESR signals at $g \approx 4.3$ decreased with increasing amount of K_2O. This signal is believed that derived from impurities, such as Fe^{3+} ion in the sample (Elvers and Weissmann, 2001). On the contrary, the intensity of the ESR

signal at g≈2.0 decreased with increase in amount of K_2O (X). However, the NIR luminescent intensity seems to be not proportion to the intensity of g≈2.0 signals of ESR spectra, this result is similar to section 4.1.
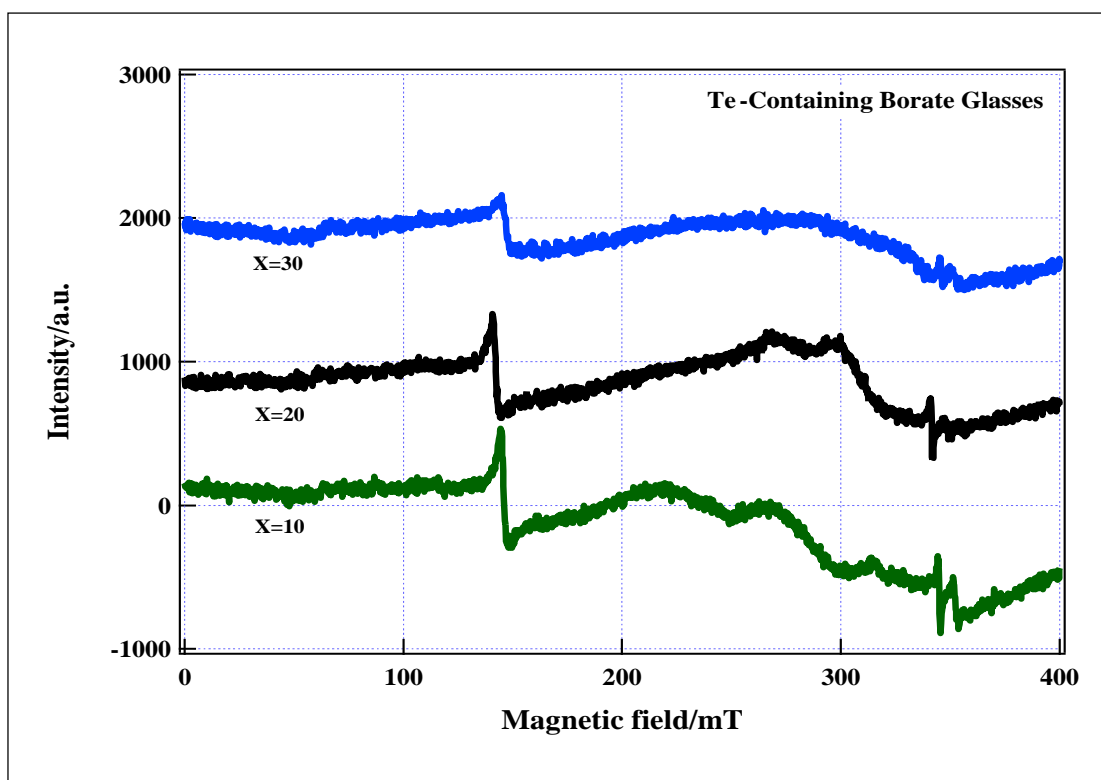
Figure 4.6 ESR spectra of Te-containing borate glasses.

4.2.1.4 XPS spectra

Figure 4.7 shows the Te 3d spin–orbit core level spectra for all glass samples investigated. It is clear that the peak intensity decreases with increasing K_2O content, while the peak positions remain essentially the same for all glass compositions. The binding energies (BE) of the Te $3d_{5/2}$ are measured to be ~577 eV as shown in table 4.4. The Te $3d_{5/2}$ peaks are symmetric with a full-width at half-maximum (FWHM) varying between 2.5 and 2.6 eV, the observations of the

similarities in the values for the peak position and FWHM of the Te3d core level spectra for all glass samples with those measured for the TeO_2 powder and any signal can not be observed in lower energy side of these peaks lead to the conclusion that the addition of K_2O does not result in a change of the local TeO_2 structure from the basic TeO_4 trigonal bipyramid (tbp) structural units (Mekki et al, 2006) and considerable amount of lower valence species (Te, Te_2, Te_2^-, (Te)n and Te^{2-}) is not present in these glasses.
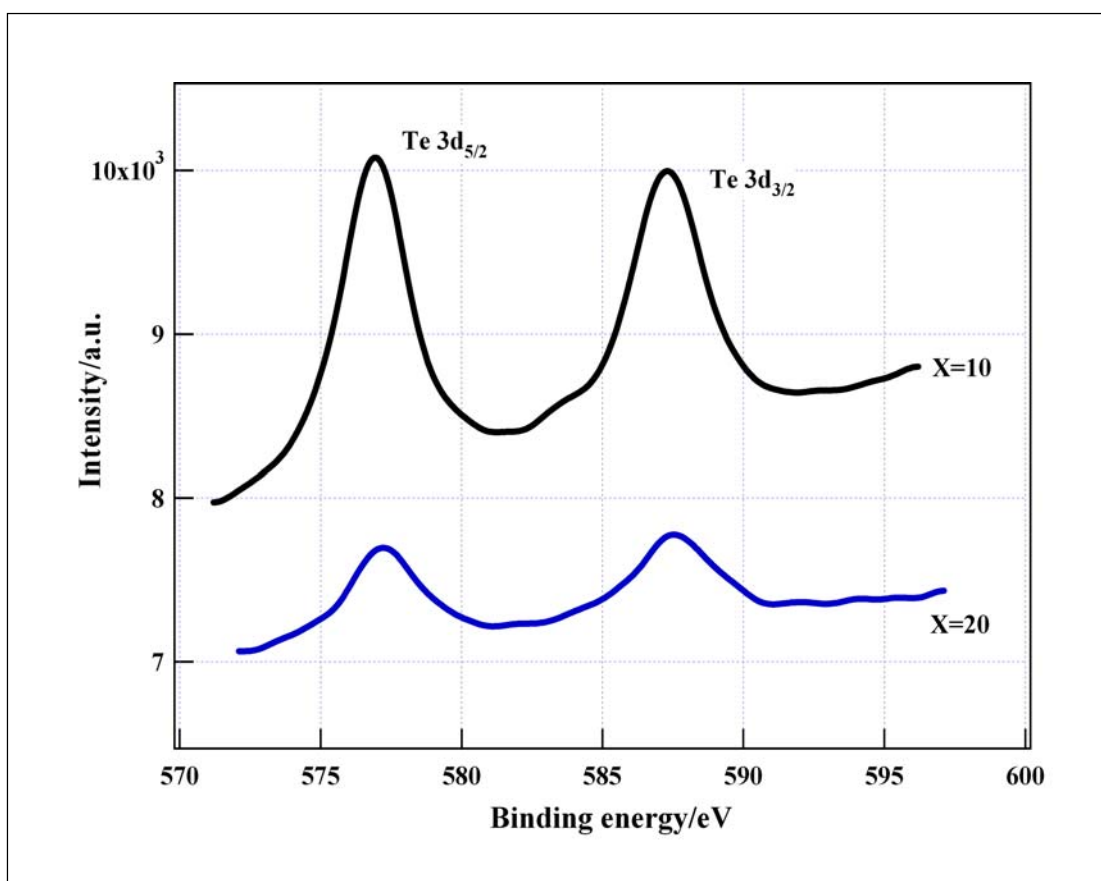
Figure 4.7 Core level Te3d spectra of Te-containing borate glasses.

Table 4.4 Peak positions in eV for the core levels Te $3d_{5/2}$ and their corresponding

FWHM (full-width at half-maximum) at different in glass

composition of Te-containing borate glasses.

Melting Temperature/°C	Te $3d_{5/2}$/eV	FWHM/eV
X=10	577.3	2.6
X=20	577.5	2.5

4.2.2 Discussion

Here, the effect of melting temperature and glass composition on the coloration and NIR luminescence of Te containing borate glasses will be discussed together.

It was found that the coloration of Te-doped borate glasses was strongly affected by melting temperature and glass composition. The color became deeper with increase in the melting temperature and decrease in the alkali content, and basically three absorption bands can be observed, ~370 nm, ~430 nm and ~530 nm, respectively. However, no NIR luminescence could be detected in all glasses unlike Bi_2O_3-containing borate glasses (Khonthon, S., et al., 2009).

According to redox equilibrium, the higher melting temperature and the lower alkali content result in lower valence state of metal ions (Paul, 1990), and hence next process may be given:

$$Te^{4+} \rightarrow Te^{2+} \rightarrow Te, Te_2, Te_2^-, etc. \rightarrow (Te)n \rightarrow Te^{2-} \tag{4.1}$$

Low ←   Melting temperature   → High
High ←   Alkali content   → Low
             (Optical basicity)

The glass melted at lower temperature (Te-850) and higher alkali containing glass (X=30) do not exhibit any characteristic absorption bands, on the contrary however, few absorption bands start to appear with increase in melting temperature and decreasing alkali content. This revealed that color centers can be formed in these glasses. Actually, three absorption bands can be detected, and these are from exciton, Te_2 and Te metallic colloid.

The spectral patterns of these glasses are different from those reported previously (ZTP, Te-SL and Te-Spinel in Table 4.1). The former three absorption bands are the same, but Band IV can not be detected in all borate glasses discussed in this study. The assignment of Band IV has already been done and is ascribed to $^2\Pi g \rightarrow ^2\Pi u$ transition of Te_2^- (Lindner et al., 1996). It is considered that the color center of Te_2^- is lacking in all borate glasses from these results. Lindner et al. (1996) reported that the absorption band due to Te_2^- appeared at 606 nm in Te-doped blue and green sodalite crystal. This position is nearly the same as those observed in ZTP, Te-SL and Te-Spinel glasses (Khonthon, S., et al., 2007). Thus, the absorption band due to Te_2^- center appeared at around 600 nm in many host materials. If Te_2^- centers are present in borate glasses, the absorption band should appear at around 600 nm. However, this bands could not be detected in all borate glasses, and therefore, it is concluded that Te_2^- center is lacking or very low concentration in borate glasses.

Te_2 or Te_2^- species may be formed during reduction process of TeO_2 to metallic colloids $(Te)n$ in glasses and they gather together and precipitate Te metallic colloids (Konishi et al., 2003). Zinc tellurium phosphate glass (ZTP) appeared to be brilliant purple and many small particles were observed by scanning electron microscope (SEM) observation in this glass (Khonthon, S., et al., 2007). These

particles were confirmed to be Te-metallic colloids and the strong absorption at around 537 nm was derived from the surface plasmon resonance absorption of Te-metallic colloids (Konishi et al., 2003). This glass contained the same amount of TeO_2 (10 mol%) as that in borate glasses and were melted at nearly the same temperature (1200°C-2h). This indicates that ZTP glass was prepared under higher reducing condition than borate glasses.

According to Duffy's optical basicity concept (Duffy, 1996), optical basicity (Λ) values for glasses were calculated without TeO_2: ZTP: 0.45, Te-SL: 0.58, Te-Spinel: 0.47 and X=0: 0.46, X=10: 0.50, X=20: 0.55 and X=30: 0.6, respectively. The Λ value of ZTP is smaller than those of borate glasses. The smaller Λ value provides in higher reducing condition, and therefore, a large amount of Te metallic colloids $(Te)n$ was formed in ZTP glass compared with borate glasses. Thus, the reduction process did not proceed enough in borate glasses and the amount of Te_2 or Te_2^- species seems to be very low. This implies the lacking or very weak absorption of Band IV in borate glasses.

NIR luminescence can not be detected in all borate glasses under the excitation of 974 nm laser diode at room temperature because of the lacking of luminescent center. It is suggested that the origin of NIR luminescence of Te-containing borate glasses is likely to be caused by Te_2^- center.

4.3 Effect of carbon addition (reducing agent) : Te-containing borate glasses

4.3.1 Results

4.3.1.1 Appearance and absorption spectra

The color changes from pale orange (C-0) to dark brown-black (C-1.0) with increase in the amount of carbon, and in C-0.5 glass, silver-white colored Te metal (4 mm diameter with 2 mm thickness) deposited during casting.

The appearance and absorption bands of these glasses are summarized in Table 4.5. Figure 4.8 shows absorption spectra of glasses. The absorption spectra for dark brown black colored glasses could not be measured. The characteristic absorption band was not observed for C-0.24, C-0.5 and C-1.0 glasses. On the other hand, three weak absorption bands can be observed at around 370 nm, 430 nm and 530 nm in C-0 glasses. The spectral pattern of C-0 glasses is quite similar to borate glasses of Te-1000~Te-1300 and X=10~X=20. Thus, it seems that the same color center is present in C-0 glasses.

Table 4.5 Appearance and absorption bands analyzed by Gaussian distribution.

Glass	Appearance	Band I	Band II	Band III	Band IV
C-0	Pale orange	370**	430	530**	–
C-0.24	Dark brown black	–	–	–	–
C-0.5	Dark brown black, Te metal	–	–	–	–
C-1.0	Dark brown black	–	–	–	–
ZTP*	Brilliant purple	375	417	537	600
Te-SL*	Pale green	374	444	526**	625
Te-Spinel*	Brownish pink	–	420 488**	556	599

Remarks: * Khonthon, S., et al. (2007), ** very weak.
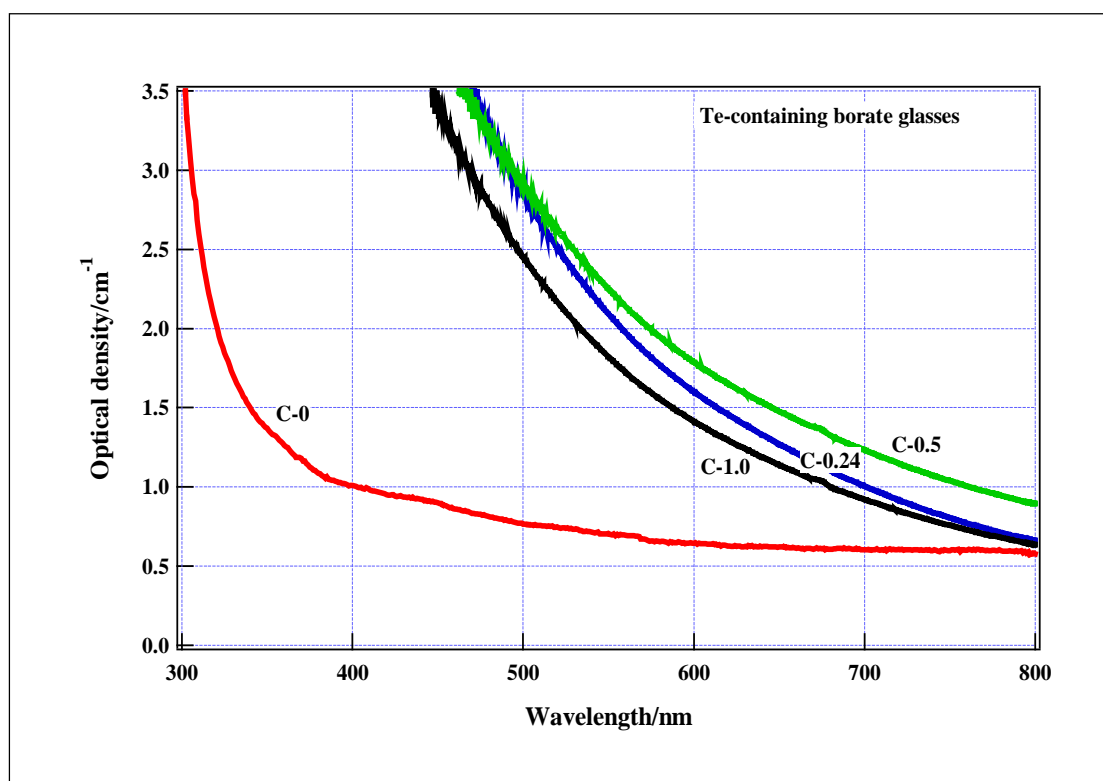
Figure 4.8 Absorption spectra of Te-containing borate glasses.

Figure 4.9 shows SEM photos of dark brown black colored glasses (C-0.24, C-0.5 and C-1.0). Many spherical particles of smaller than 0.5 μm are observed and these particles must be Te metallic colloid

Figure 4.10 shows XRD patterns of C-0.5 glasses. These XRD patterns were obtained by very slow step scan method. The diffraction peak can be detected at $2\theta = 27.9°$ and $2\theta = 38.75$, these peaks are assigned to (101) and (102) planes of Te metal (JCPDS 00-003-0506). Therefore, it is concluded that the particles observed in SEM photos could be Te metallic colloid that means TeO_2 reduced to Te metallic colloid by higher reducing condition. However, it is considered that the amount of metallic Te colloids might be very low, less than 1 wt%.
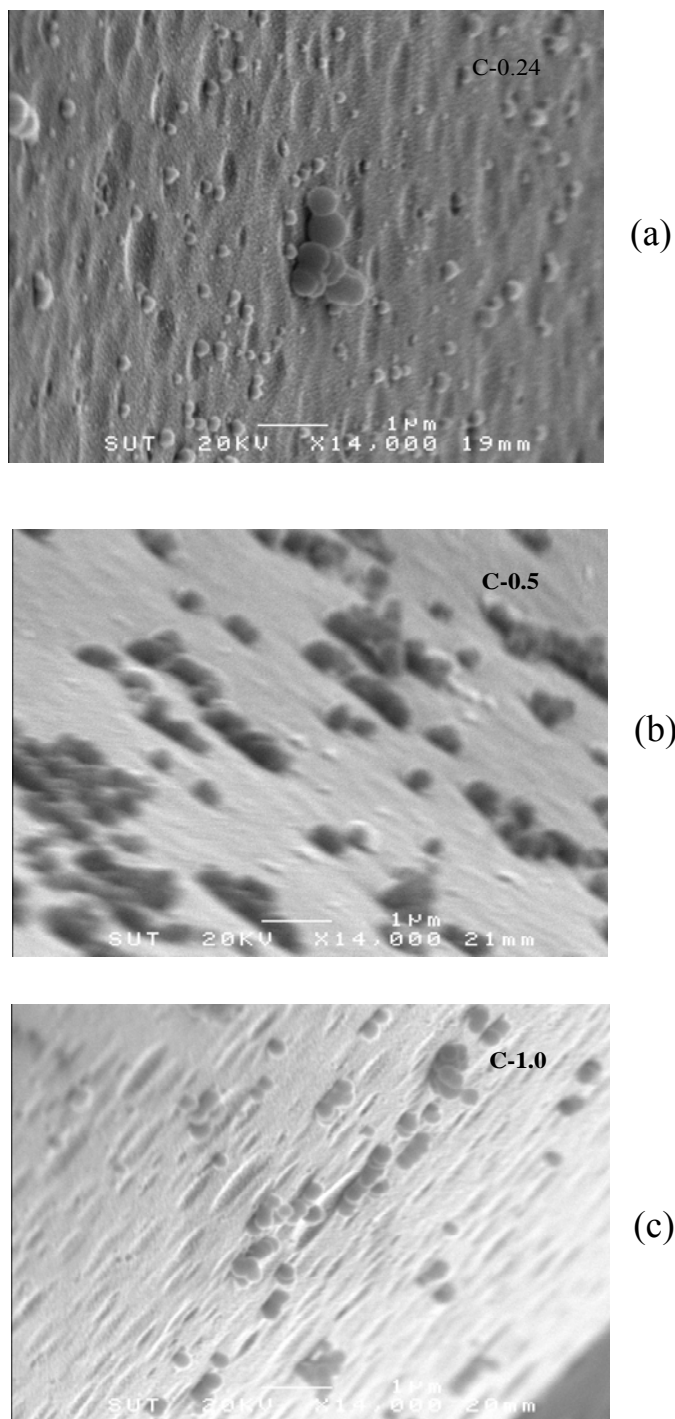
Figure 4.9 SEM photo of dark brown black of Te-containing borate glasses.

(a) 0.24 wt% of carbon addition,

(b) 0.5 wt% of carbon addition,

(c) 1.0 wt% of carbon addition
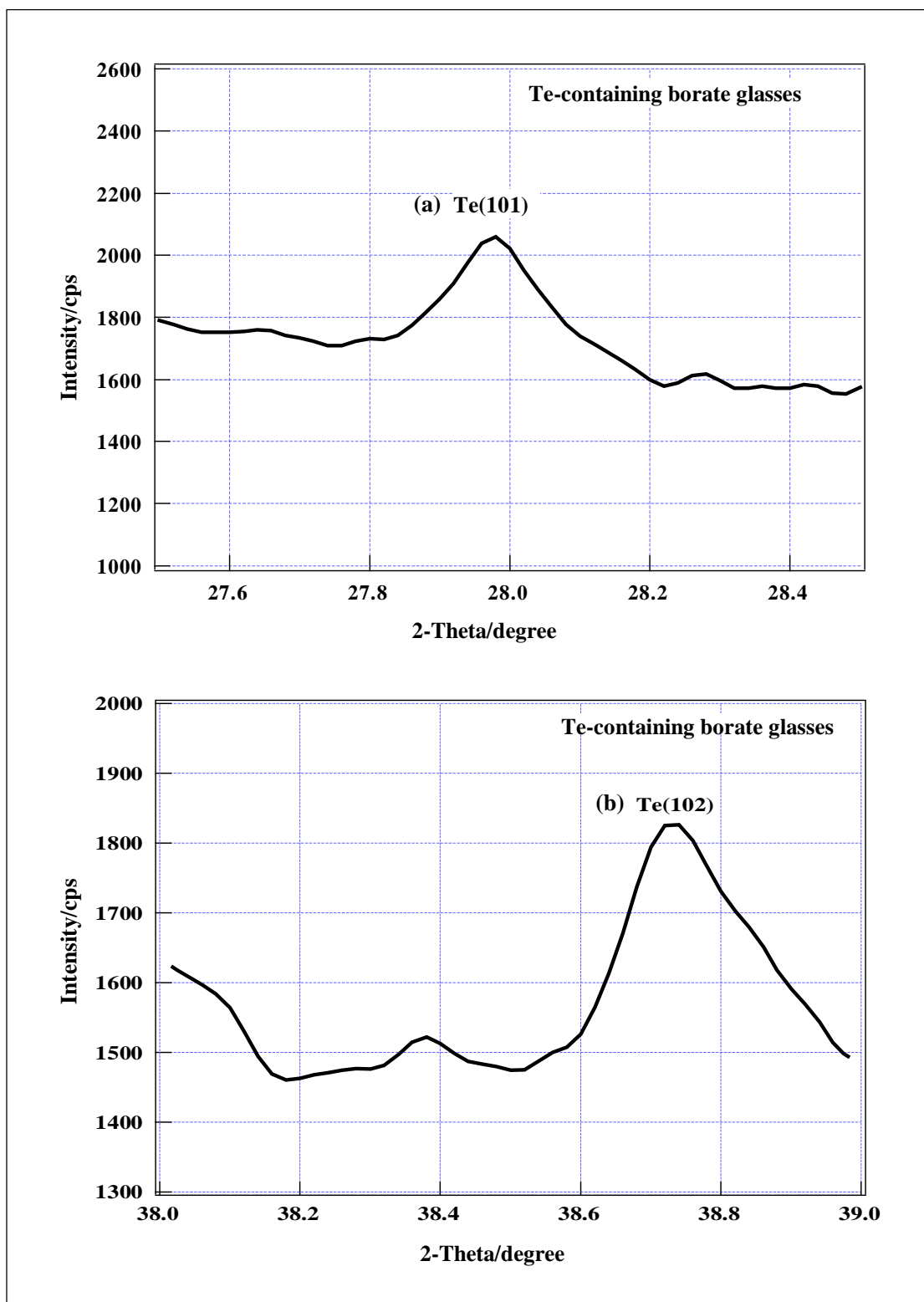
Figure 4.10 XRD patterns of Te-containing borate glass; C-0.5 glasses ((a)-(b)).

4.3.1.2 Near Infrared (NIR) luminescence

The NIR luminescence can not be detected in all borate glasses under the excitation of 974 nm laser diode at room temperature.

4.4 Effect of carbon addition (reducing agent) : Te-doped soda-lime-silicate glasses

4.4.1 Results

4.4.1.1 Appearance and absorption spectra of glasses

The appearances of these glasses change from colorless (C-0) to dark green-black (C-1.0) with increase in the amount of carbon addition. Appearances and absorption bands of these glasses are summarized in Table 4.6.

Table 4.6 Appearance and absorption bands analyzed by Gaussian distribution.

No.	Appearance	Absorption bands/nm			
		I	II	III	IV
C-0	Colorless	–	–	–	–
C-0.1	Pale green	–	–	–	–
C-0.2	Green	377**	432	–	638**
C-0.3	Green	327	435	–	633
C-0.5	Dark green	355	436	–	638
C-1.0	Dark green-black	375	438	–	634
Te-1200	Reddish orange	370	430	530	–
Te-SL*	Pale green	374	444	526**	625

Remarks: * Khonthon, S., et al. (2007), ** very weak.

Figure 4.11 shows absorption spectra of these glasses. Three absorption bands can be observed in C-0.2, C-0.3, C-0.5 and C-1.0 glasses, 330~380 nm, ~430 nm, ~630 nm, respectively. The intensity of absorption bands increases with increase in the amount of carbon, and the absorbance is high in whole wavelength region in C-0.5 and C-1.0 glasses. For green Te-doped soda-lime-silicate glasses, the absorption band at 330~380 nm band may relate to exciton transition (Lindner et al., 1996), the absorption band at 430 nm is ascribed to $^3\Sigma g \rightarrow {}^3\Sigma u$ transition of Te_2 color center and the absorption band at 625 nm can be assigned to $^2\Pi g \rightarrow {}^2\Pi u$ transition of Te_2^- color center (Lindner et al., 1996). The absorption band at 530 nm can not be detected in theses glasses.
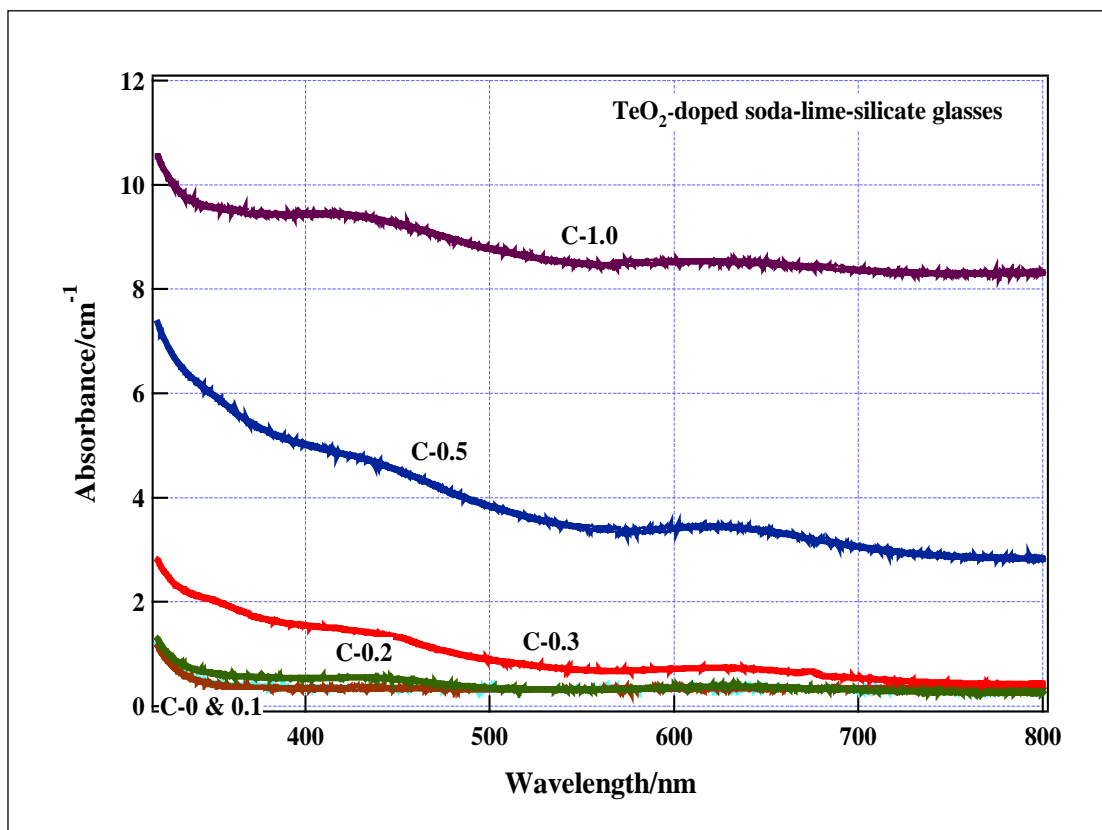
Figure 4.11 Absorption spectra of Te-containing soda-lime-silicate glasses.

4.4.1.2 Near Infrared (NIR) luminescence

Figure 4.12 shows the NIR luminescence spectra of glasses under the excitation of 974 nm laser diode at room temperature. In these glasses, the strong and broad emission band can be observed at around 1200 nm except for glasses of lower carbon addition (C-0, C-0.1 and C-0.2 glasses). The luminescent intensity increases with increase in the amount of carbon and reaches to the maximum at C= 0.5 wt% and decrease slightly again at C= 1.0 wt% as shown in Figure 4.13.
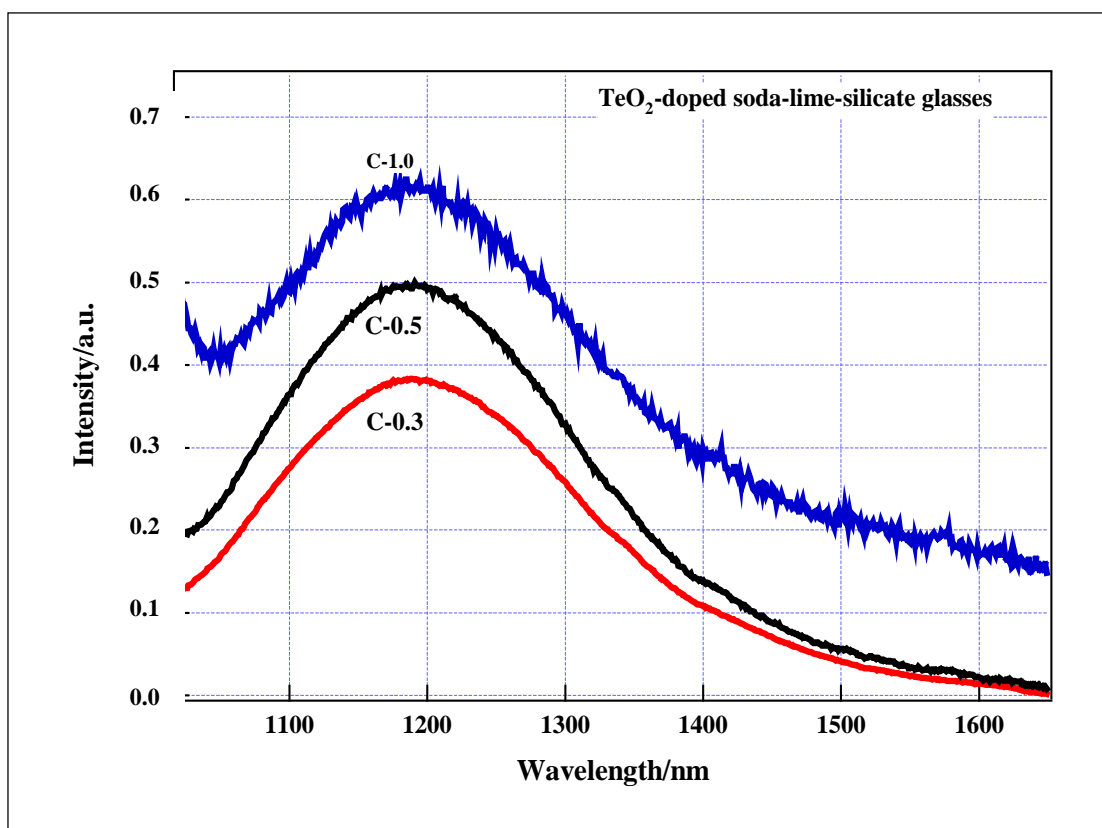
Figure 4.12 NIR luminescence spectra of Te-containing soda-lime-silicate glasses under the excitation of 974 nm laser diode.
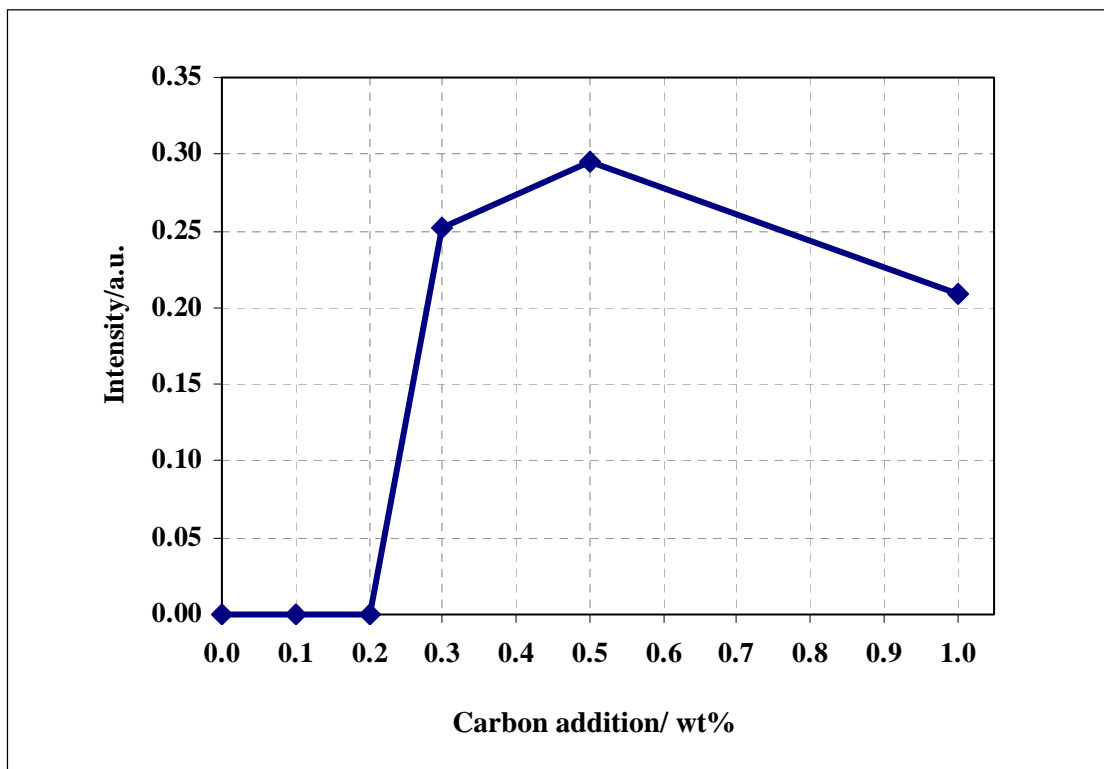
Figure 4.13 The relation of NIR luminescence intensity and the amount of carbon (wt%) of Te-containing soda-lime-silicate glasses.

4.5 Effect of TeO₂ concentration : Te-doped soda-lime-silicate glasses

4.5.1 Results

4.5.1.1 Appearance and absorption spectra of glasses

The colors of glasses change from green (Te-0.2) to pale green (Te-2.0) with increase in TeO_2 concentration. Appearances and absorption bands of these glasses are summarized in Table 4.7.

Table 4.7 Appearance and absorption bands analyzed by Gaussian distribution.

No.	Appearance	Absorption bands/nm			
		I	II	III	IV
Te-0.2	Green	367	437	–	635
Te-0.5	Green, partly brownish green	344	432	–	633
Te-0.7	Green, partly brownish green	349	435	–	634
Te-1.0	Green	327	435	–	633
Te-2.0	Pale Green	331	436	–	633
Te-1200	Reddish orange	370	430	530	–
Te-SL*	Pale green	374	444	526**	625

Remarks: * Khonthon, S., et al. (2007), ** very weak.

Figure 4.14 shows absorption spectra of these glasses. Three absorption bands can be observed in all glasses, 330~380 nm, ~430 nm, ~630 nm, respectively. These spectral patterns are similar to those glasses in the last section. In these glasses, the intensity of absorption bands increases with increase in the amount of TeO_2 (0.2-1.0 wt%) and decreases again. However, the absorption band owing to Te-metallic colloids (~530 nm) can not be observed in all glasses discussed here. The assignment of these absorption bands has been already known that the absorption band at 330~380 nm band may relate to exciton transition (Lindner et al., 1996), the absorption band at 430 nm is ascribed to $^3\Sigma g \rightarrow {}^3\Sigma u$ transition of Te_2 color center and the absorption band at 625 nm can be assigned to $^2\Pi g \rightarrow {}^2\Pi u$ transition of Te_2^- color center (Lindner et al., 1996).
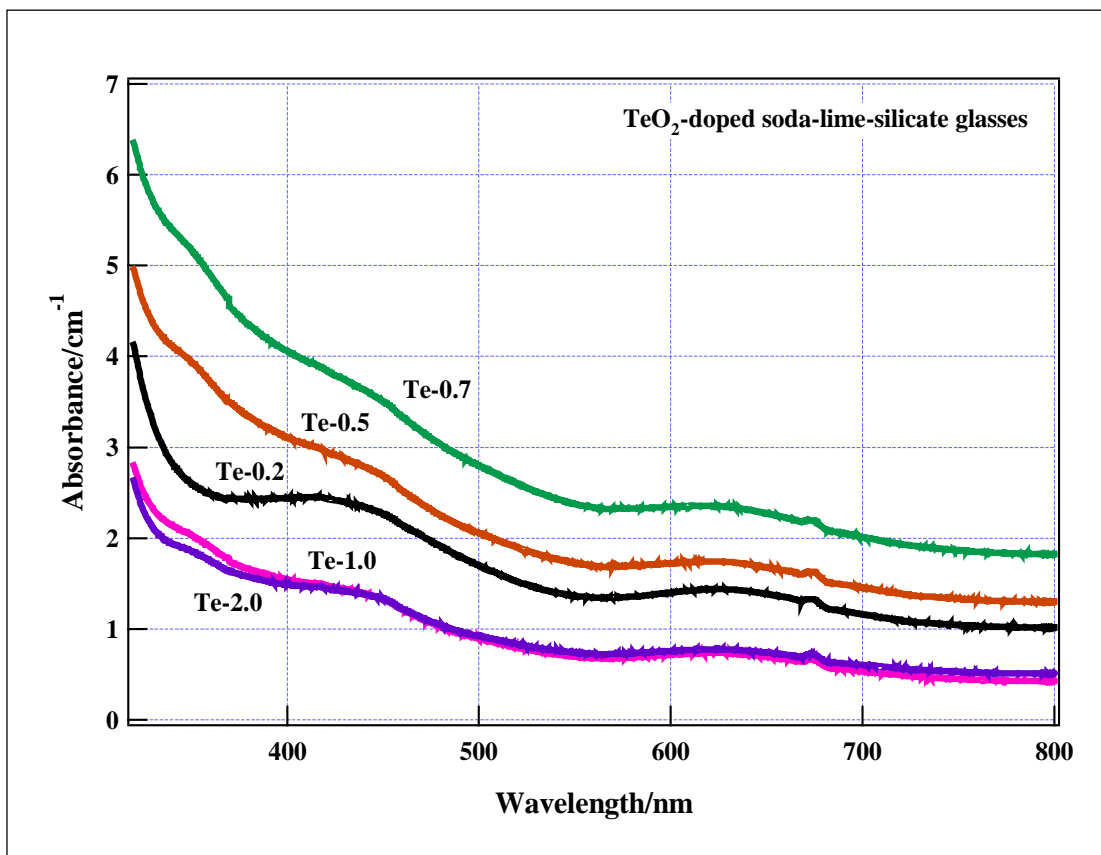
Figure 4.14 Absorption spectra of Te-containing soda-lime-silicate glasses.

4.5.1.2 Near Infrared (NIR) luminescence

Figure 4.15 shows the NIR luminescence spectra of glasses under the excitation of 974 nm laser diode at room temperature. The emission band can be observed at around 1200 nm in all of these glasses, the luminescent intensity increases with increase in TeO_2 concentration and reaches to the maximum at TeO_2 = 1.0 wt% and decrease slightly again at TeO_2 = 2.0 wt% (Figure 4.16). Thus the intensity of NIR luminescence was strongly affected by TeO_2 concentration.
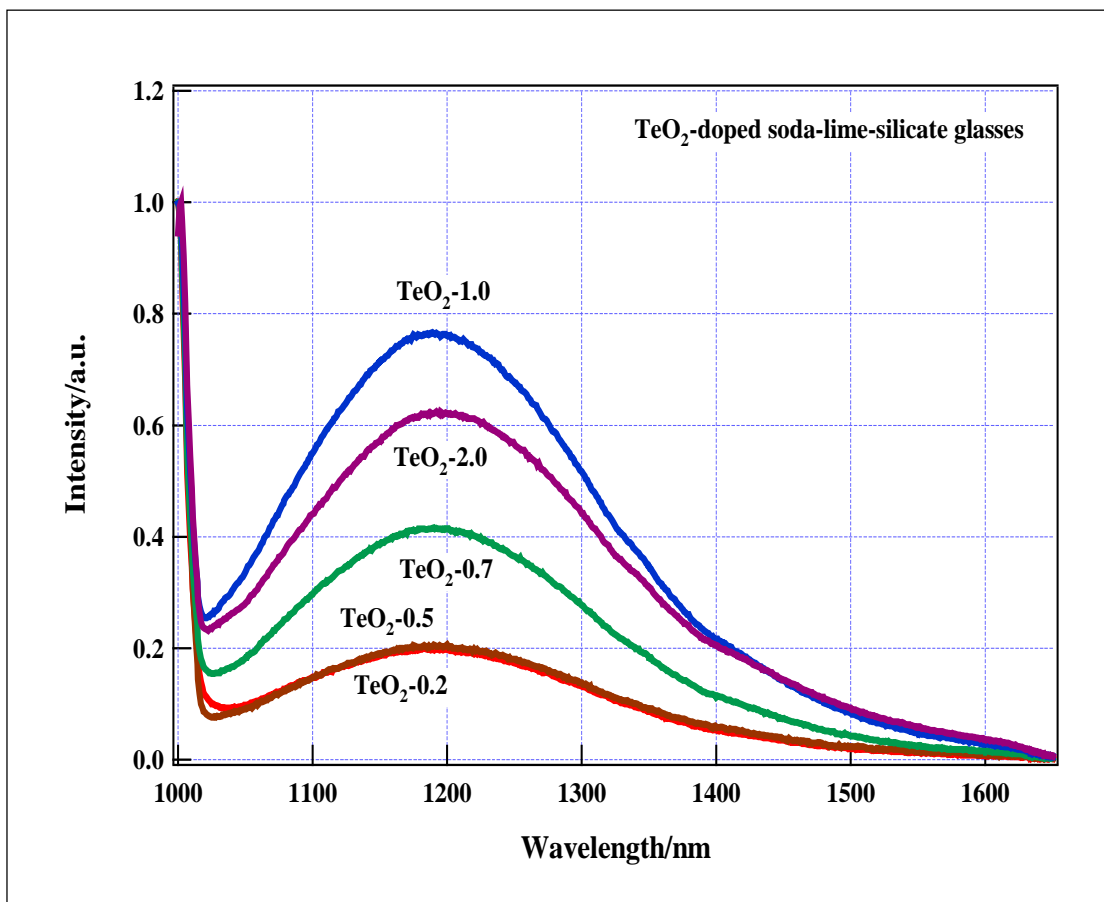
Figure 4.15 NIR luminescence spectra of Te-containing soda-lime-silicate glasses

under the excitation of 974 nm laser diode.
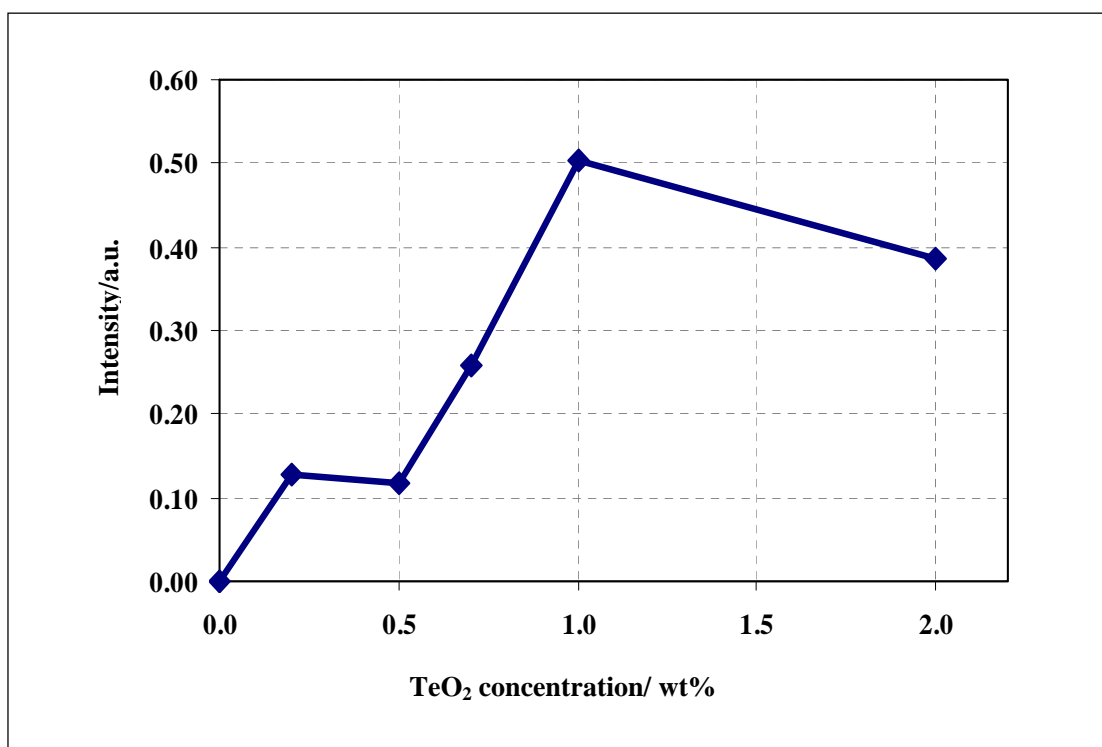
Figure 4.16 The relation of NIR luminescence intensity and the TeO_2 concentration

(wt %) of Te-containing soda-lime-silicate glasses.

4.5.2 Discussion

4.5.2.1 Effect of carbon addition

The reducing agent such as carbon affects directly to the redox equilibrium of opponent oxides (Paul, 1990), the concentration of lower valence state of Te species increases with increase in the amount of reducing agent (carbon). Here, the effect of carbon addition on the absorption spectra and NIR luminescence of soda-lime-silicate glass is discussed.

As mentioned previously, the basicity of glasses strongly affected to absorption spectra and NIR luminescence characteristics of glasses. The optical basicity of soda-lime silicate glass discussed here (without carbon) is

calculated to be Λ=0.58, which is much greater than the critical value of 0.4 (Murata and Mouri, 2007), and hence the NIR luminescence could not be detected in C-0, C-0.1 and 0.2 glasses even melted at 1450°C. The NIR luminescence started to appear at C-0.3 and the luminescent intensity increases with increase in the amount of carbon and reaches to the maximum at C=0.5 wt% (intensity=0.3 a.u.) and decrease slightly again at C=1.0 wt%.

The weak absorption band at around 630 nm due to Te_2^- species disappeared in C-0~C-0.2 glasses and the NIR luminescence can not be detected from these glasses. This suggests that there is a limited concentration of luminescent center for the generation of NIR luminescence, and the concentration of luminescent center in these glasses (C-0~C-0.2) is not high enough and NIR luminescence might not appear. It seems that the concentration of luminescent center might be very low, ppm order.

4.5.2.2 Effect of TeO_2 concentration

In soda-lime silicate glass, the absorption band at around 630 nm due to Te_2^- species appears and NIR luminescence can be detected. On the contrary in borate glass, both the absorption band at around 630 nm and the NIR luminescence can not be observed. Here, the effect of TeO_2 concentration on the NIR luminescence is discussed in combination with carbon addition.

The NIR luminescence intensity increases with increasing TeO_2 concentration and reaches the maximum at TeO_2=1wt% (intensity=0.5 a.u.) and then decreases again at fixed amount of carbon addition, 0.3 wt%, in soda-lime silicate glasses. It is clear that the C/TeO_2 ratio also affects to the formation of luminescent center. This result indicates that the ratio of C/TeO_2=0.3 might be suitable. Further

increase in the amount of TeO_2, $C/TeO_2=0.15$ is not enough for the formation of luminescent center. Thus, the milder reducing condition enhances the NIR luminescent intensity of TeO_2 doped soda-lime-silicate glass.

In borate glasses, NIR luminescence could not be detected. The optical basicity of borate glass is calculated to be $\Lambda=0.55$ according to Duffy's scheme, which is also greater than the critical value of 0.4 (Murata and Mouri, 2007). Therefore, borate glass without carbon did not exhibit NIR luminescence. However, glasses appear to be brown to black color (borate, C-0.24~1.0) and finally Te metal deposited (borate, C-0.5) by the addition of carbon. This phenomenon may be the process III in next equation. Atomic or molecular Te gathers together, grows and forms Te metallic colloids. This process is often observed in the formation process of noble-metal colloid (Rawson, 1980).

$$\text{[I]} \qquad \text{[II]} \qquad\qquad \text{[III]}$$
$$Te^{4+} \rightarrow Te^{2+} \rightarrow Te, Te_2, Te_2^-, \text{ etc.} \rightarrow (Te)n \rightarrow Te^{2-} \tag{4.2}$$
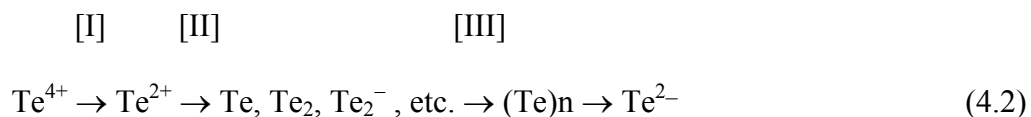
In fact, many particles were observed in C-0.24-C-1.0 borate glasses. On the contrary, no such phenomenon was observed in soda-lime-silicate glass. The most significant difference between borate glass and soda-lime-silicate glass is the concentration of TeO_2. The borate glass contains about 19 wt% of TeO_2, but soda-lime-silicate glass contains only 1 wt% of TeO_2. Thus, carbon reduces TeO_2 to Te atoms or molecules, the concentration of these species becomes to be high and they gather together, grow and form Te metallic colloids in borate glass. However, it is considered that the concentration of the Te atoms or molecules in soda-lime-silicate glass is not high, probably below solubility limit, and hence they are more stable than

in borate glass. And finally, the color center and luminescent center of Te_2^- were formed in soda-lime-silicate glass, and the absorption band and NIR luminescence appear.

Consequently, it is suggested that the different system of glass might be suitable for generated NIR luminescence in the different of reducing condition and the origin of NIR luminescence of Te-containing borate glasses is likely to be caused by Te_2^- center.

4.6 Structure and properties of TeO$_2$- containing borate glasses

4.6.1 Results

4.6.1.1 Appearance and properties of glasses

The properties of glasses are summarized in Table 4.8. Though Te-0 glass exhibits slight opaque because of phase separation, other glasses show pale yellow to pale brown.

Table 4.8 Properties of TeO$_2$- containing borate glasses.

Glass	Appearance	Thermal properties			Density g/cm^3	Molar volume cm^3/Mol
		Tg/°C	Td/°C	$\alpha/10^{-7}\cdot K^{-1}$		
Te-0	Slightly opaque*	512	–	–	2.154	34.44
Te-10	Pale yellow	452	503	101.2	2.445	33.78
Te-20	Pale brown	396	453	93.6	2.817	32.37
Te-30	Pale brown	366	**	**	3.172	31.44

Remarks: * Slightly phase separation, ** can not be measured by dilatometer

Figure 4.17 shows the composition dependence of glass transition temperature. The glass transition temperature decreases linearly with increase in X.

Figure 4.18 shows the density and molar volume of glasses as a function of glass composition. Molar volume may be calculated as follows:

$$\text{M.V.} = \text{Molar weight/density (cm}^3\text{/Mol)} \tag{4.3}$$

The density increases linearly with increase in X, on the contrary, molar volume shows different manner of change. The molar volume of TeO_2-containing borate glasses decreases almost linearly with increase in X. The density and molar volume of crystalline $\alpha-TeO_2$ (para-tellurite) are also shown in these figures. By extrapolation of density and molar volume to 100% of TeO_2 (para-tellurite crystal), a good linearity can be obtained.
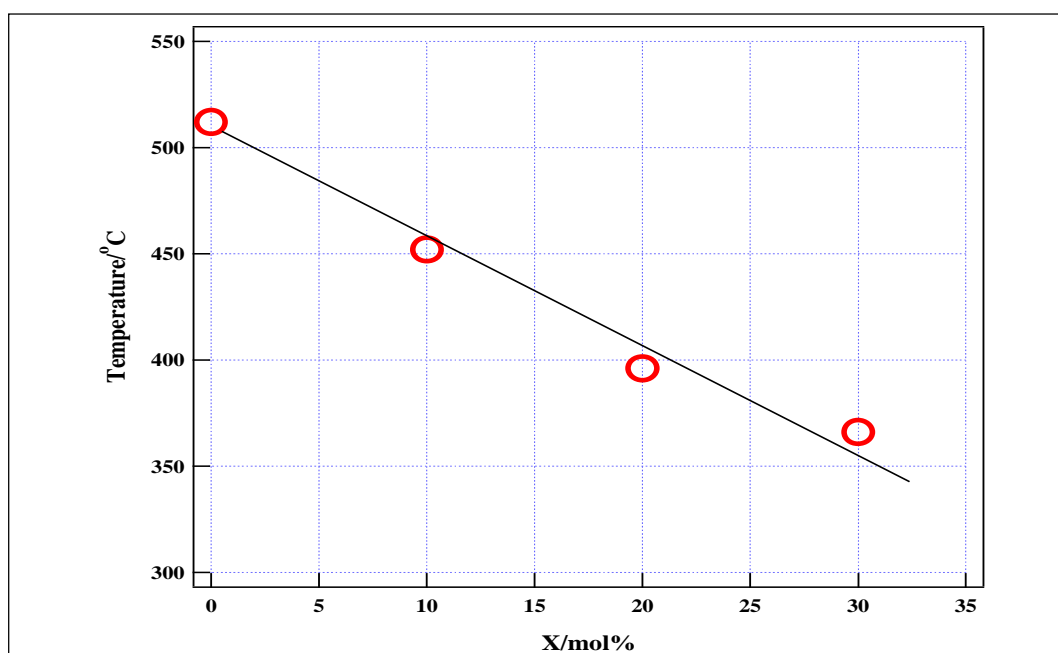
Figure 4.17 The relation of glass composition and glass transition temperature.
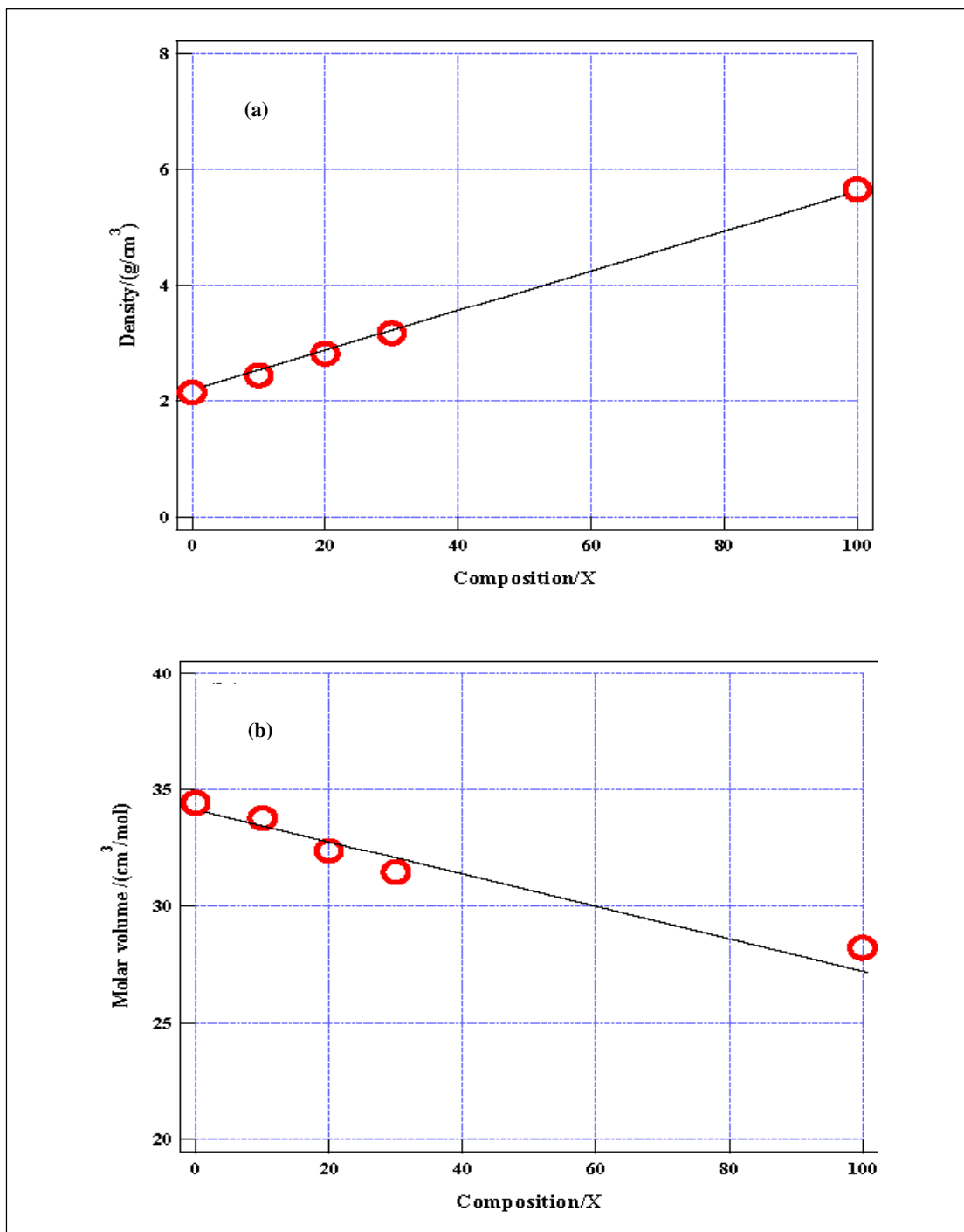
Figure 4.18 Properties of TeO$_2$–containing B$_2$O$_3$-Al$_2$O$_3$-ZnO glasses.

(a) The density of glasses as a function of glass

composition, (b) Molar volume of glasses

as a function of glass composition

4.6.1.2 X-ray absorption spectra

Figure 4.19 compares the Te L_{III} edge normalized XANES spectra of Te-containing borate glasses $(100-X)[80B_2O_3 \cdot 10Al_2O_3 \cdot 10ZnO] \cdot XTeO_2$ of various compositions with the references TeO_2 (para-tellurite). The pre peak was observed at around 4345.5 eV for all glasses and TeO_2 standard (para-tellurite). The peak position does not change, but the peak intensity changes. The XANES spectra show that the valence state of Te ions was basically 4 in all glasses. For crystalline para-tellurite, this pre-peak looks like shoulder, however, this pre-peak becomes to be more clear and distinct in glasses.
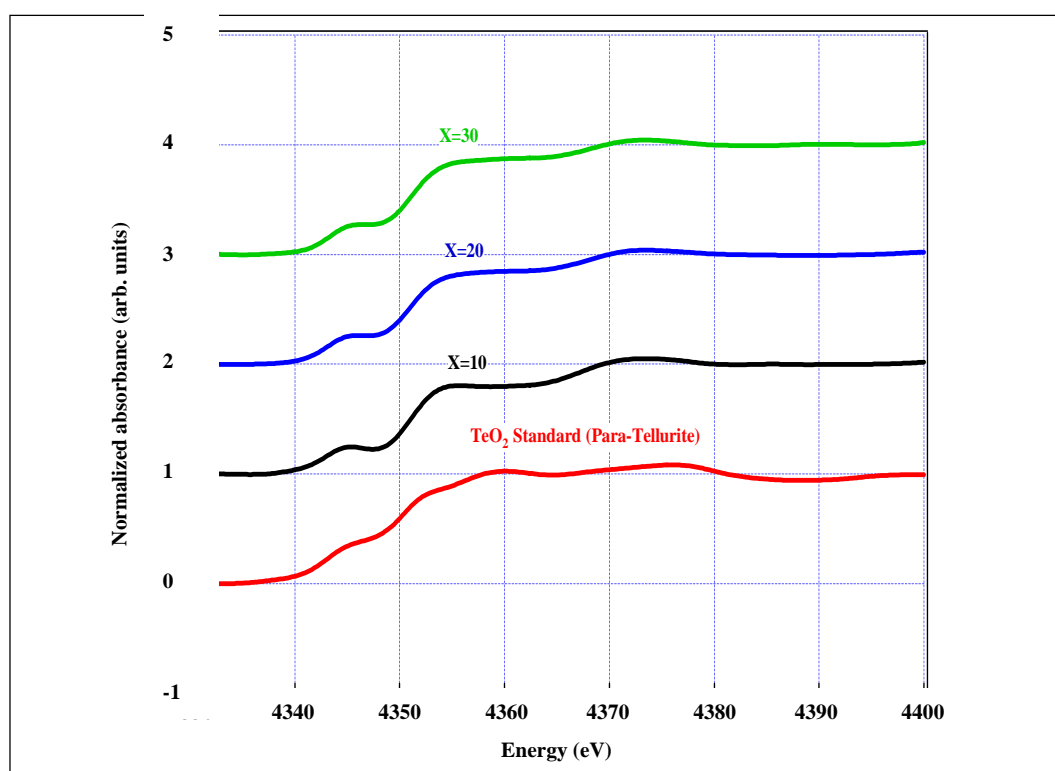
Figure 4.19 Normalized Te–L_{III} edge XANES spectra of Te-containing borate glasses

$(100-X)[80B_2O_3 \cdot 10Al_2O_3 \cdot 10ZnO] \cdot XTeO_2$ (mol%, X=0, 10, 20 and 30)

and reference crystals.

4.6.2 Discussion

TeO$_2$ can not be formed as a glass by itself and is not pure glass forming oxides unlike SiO$_2$, B$_2$O$_3$, etc. However, the addition of slight amount of second oxides leads to be formed as a glass. Thus, TeO$_2$ can be regarded as pseudo glass forming oxide. On the contrary, borate glasses often show boric oxide anomaly, which shows the minimum or maximum in relation between properties and composition by adding modifier oxides. In these glasses, no abnormal change in properties was observed, and hence TeO$_2$ are incorporated into B$_2$O$_3$ network structure gradually. It was found that the glass transition temperature (Tg) decreases monotonically with increase in the amount of TeO$_2$. The density and molar volume also increases and decreases gradually with increasing amount of TeO$_2$. This reveals that TeO$_2$ is incorporated into borate structure as a glass former.

XANES spectra indicates that TeO$_4$ trigonal bipyramids structural units present uniformly in these glasses and this structural unit shares corners with BO$_3$ and BO$_4$ structural units. In crystalline $\alpha-$TeO$_2$ (para-tellurite), TeO$_4$ trigonal bipyramidal structural unit shares their corners and forms three dimensional structure (Wells, 1975). This trigonal bipyramids structural unit is converted to trigonal pyramids by the addition of modifier oxides (Sabadel et al., 1999; Charton et al., 2002a; 2004b). Thus, the pre-peak in XANES spectra becomes to be more clear and distinct, in figture 4.21 shows the zoom pre-edge of normalized Te L$_{III}$ edge XANES spectra of (a) (1-x) TeO$_2$–xWO$_3$ glasses with the references. (Sabadel et al., 1999; Charton et al., 2002a; 2004b).
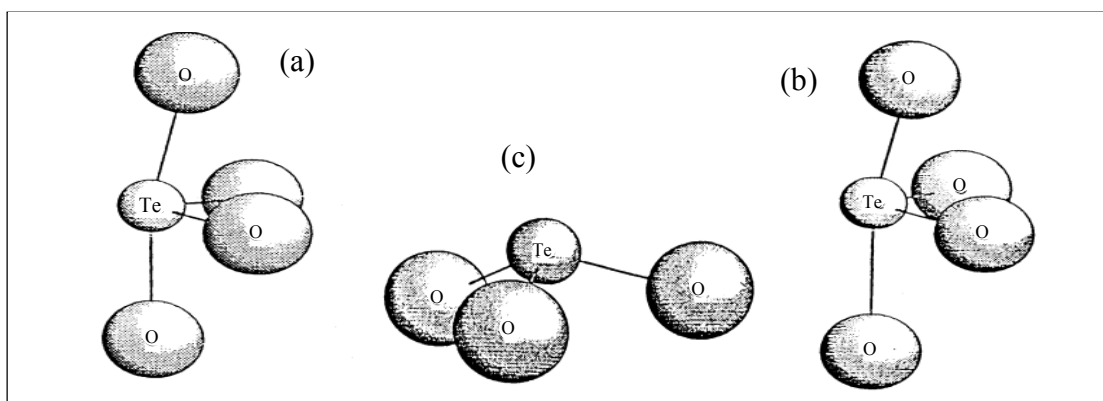
Figure 4.20 Illustration of the tellurium atom coordination by oxygen :

(a) TeO_4 trigonal bipyramid tbp, (b) TeO_{3+1} polyhedron,

(c) TeO_3 trigonal pyramid (tp) (Berthereau et al, 1996).
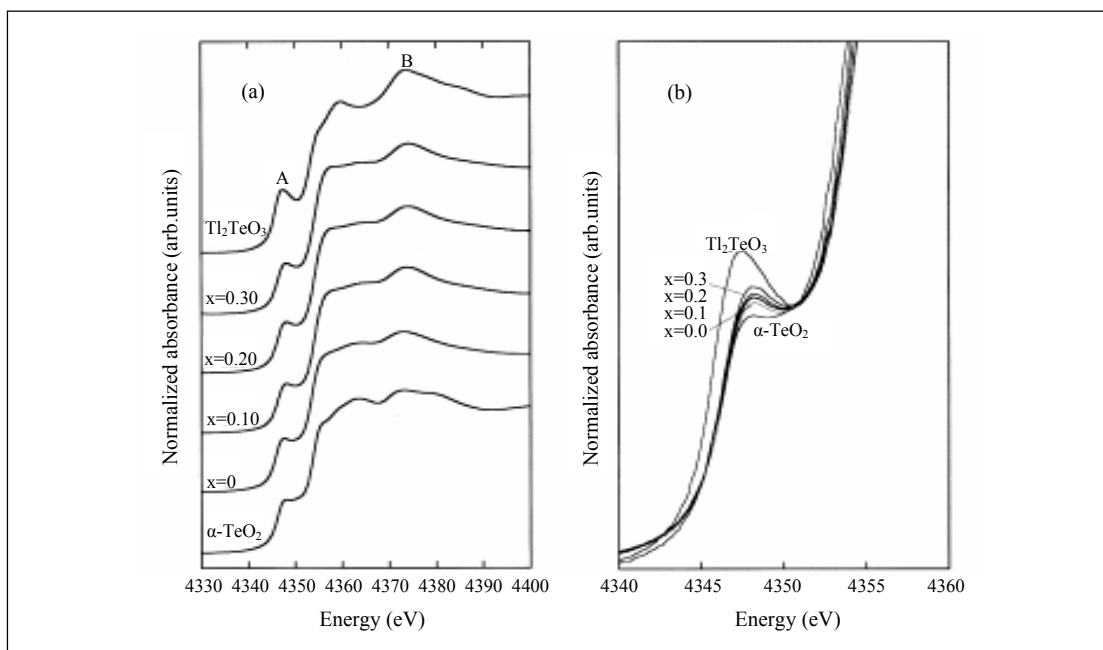
Figure 4.21 Normalized Te-L_{III} edge XANES spectra of (a) $(1-x)TeO_2–xWO_3$ glasses

with the references Tl_2TeO_3 and α-TeO_2. In (b), zoom of the pre-edge

feature A. (Charton et al., 2002).

However, in B_2O_3-Al_2O_3-ZnO-TeO_2 glasses, the amount of modifier oxide is only 10 mol% and Al_2O_3 are present. Therefore, the amount of non-bridging oxygen ions must be the minimum, and TeO_2 incorporated might not form trigonal pyramid. TeO_4 trigonal bipyramids structural unit disperses uniformly in B_2O_3 structural network and forms isolated TeO_4 and they share corners with BO_3 or BO_4 structural units. It seems that the intensity of pre-peak might increases.

CHAPTER V

CONCLUSION

NIR luminescent characteristics of Te-doped glasses were investigated based on redox equilibrium. Particularly, the factors affecting the redox equilibrium i.e. melting temperature, carbon addition and glass composition of borate glasses, and carbon addition and Te concentration of soda-lime-silicate glasses were investigated, and the formation of color center and NIR luminescent center was discussed.

5.1   Effect of melting temperature : Te-containing borate glasses

1. It was found that the coloration of Te-doped borate glasses was strongly affected by melting temperature. The color became deeper with increase in melting temperature. The glass melted at lower temperature not exhibit any characteristic absorption bands, color center and NIR luminescent center were not formed. On the contrary however, color centers can be formed in these glasses and few absorption bands start to appear with increase in melting temperature. Actually, three absorption bands can be detected, and these are from exciton, Te_2 and Te metallic colloid.

2. The reduction process did not proceed enough in borate glasses and the amount of Te_2 or Te_2^- species seems to be very low. This implies the lacking or very weak absorption of Band IV in borate glasses.

3. NIR luminescence can not be detected in all borate glasses under the excitation of 974 nm laser diode at room temperature because of the lacking of luminescent center at around 600 nm. It is suggested that the origin of NIR luminescence of Te-containing borate glasses is likely to be caused by Te_2^- center.

5.2   Effect of glass composition : Te-containing borate glasses

1. It was found that the coloration of Te-doped borate glasses was strongly affected by glass composition. The color became deeper with decrease in the alkali content.

2. The color center and NIR luminescence center disappeared with increase in the amount of alkali content (increase in basicity of glass). The color center and NIR luminescent center were not formed and NIR luminescence could not be detected in all borate glasses.

3. The formation of color center and NIR luminescent center and NIR luminescence characteristics were discussed based on optical basicity scheme (measure of basicity of glasses, Λ). The smaller Λ value was given in higher reducing condition and the lower alkali content results in lower valence state of metal ions, in borate glasses, the reduction process did not proceed enough and the amount of Te_2 or Te_2^- species seems to be very low. This implies the lacking or very weak absorption of Band IV in borate glasses.

5.3 Effect of carbon addition (reducing agent) : Te-containing borate glasses

1. It was found that the addition of reducing agent also affected the formation of the color center and the NIR luminescence center and NIR luminescence characteristics.

2. NIR luminescence can not be detected in all borate glasses under the excitation of 974 nm laser diode at room temperature.

3. Te-containing borate glasses appear to be brown to black color and finally Te metal deposited by the addition of carbon and many spherical particles were observed by SEM observation of black colored glasses. Thus, the color center and NIR luminescence can not be detected in all glasses.

5.4 Effect of carbon addition (reducing agent) : Te-doped soda-lime-silicate glasses

1. It was found that the addition of reducing agent also affected the formation of the color center and the NIR luminescence center and NIR luminescence characteristics in soda-lime silicate glasses.

2. The NIR luminescence can be observed at around 1200 nm except for glasses of lower carbon addition. The NIR luminescence started to appear at carbon 0.3 wt% and the luminescent intensity reaches to the maximum at C= 0.5 wt%. It is found that the ratio of $C/TeO_2=0.5$. However, the luminescent intensity of this glass is measured to be 0.3 a.u. which is smaller than ratio of $C/TeO_2=0.3$ of glass sample in section 5.5.

3. It was found that the soda-lime-silicate glasses have a limited concentration of luminescent center for the generation of NIR luminescence. In glasses of lower carbon addition the concentration of luminescent center is not high enough. Therefore, NIR luminescence does not appear. It seems that the concentration of luminescent center might be very low, ppm order.

5.5   Effect of TeO_2 concentration : Te-doped soda-lime-silicate glasses

1. The absorption band at around 630 nm due to Te_2^- species appears and NIR luminescence can be detected in soda-lime-silicate glasses.

2. The C/TeO_2 ratio also affects to the formation of luminescent center. It is found that the ratio of $C/TeO_2=0.3$ might be suitable. Further increase in the amount of TeO_2, $C/TeO_2=0.15$ is not enough for the formation of luminescent center. Thus, the milder reducing condition enhances the NIR luminescent intensity of TeO_2 doped soda-lime-silicate glass.

3. The concentration of the Te atoms or molecules in soda-lime-silicate glass is not high, probably below solubility limit, and hence they are stable. And finally, the color center and luminescent center of Te_2^- were formed in soda-lime-silicate glass, and the absorption band and NIR luminescence appear. It is suggested the origin of NIR luminescence of Te-containing soda-lime-silicate glasses is likely to be caused by Te_2^- center.

5.6 Structure and properties of TeO$_2$- containing borate glasses

1. It was found that the glass transition temperature (Tg) decreases monotonically with increase in the amount of TeO$_2$.

2. The density and molar volume also increases and decreases gradually with increasing amount of TeO$_2$. This reveals that TeO$_2$ is incorporated into borate structure as a glass former.

3. XANES spectra indicates that TeO$_4$ trigonal bipyramids structural units present uniformly in these glasses.

It was found that the formation of color center and NIR luminescent center and luminescent characteristic of Te- containing glasses were strongly affected by redox equilibrium, glass composition, melting temperature and addition of reducing agent. In oxidized side, color center and NIR luminescent center were not formed, and hence NIR luminescence could not be detected. On the contrary, glasses appear to be brown to black color and finally Te metal deposited in borate glasses (formation process of Te metallic colloids) in strong reduced side and also NIR luminescence was not observed.

Consequently, NIR luminescence can be obtained under the mild to medium reducing atmosphere, and the origin of NIR luminescence of Te-containing glasses is likely to be caused by Te$_2^-$ center.

REFERENCES

Ahmed, A.A., Sharaf, N.A., and Codrate Sr., R.A. (1997). Raman microprobe investigation of sulfur-doped alkali borate glasses. **Journal of Non-Crystalline Solids.** 210: 59-69.

Albrecht, G.F., Eggleston, J.M., and Ewing, J.J. (1985). Measurements of Ti^{3+}:Al_2O_3 as a lasing material. **Optics Communications.** 52: 401-404.

Branda, F., Buri, A., Marotta, A., and Saiello, S. (1984). Glass transition temperature and devitrification behaviour of glasses in the $Na_2O\cdot2SiO_2$-$BaO\cdot2SiO_2$ composition range. **Journal of Materials Science Letters.** 3: 654-658.

Bates, T. (1994). Ligand Field Theory and Absorption Spectra of Transition-Metal Ions in Glasses. In J.D. Butterworth (ed.). **Modern Aspects of the Vitreous State Vol. II** (pp. 195-254). London: Mackenzie.

Charton, P., Gengembre, L., and Armand, P. (2002). TeO_2–WO_3 glasses: infrared, XPS and XANES structural characterizations. **Journal of Solid State Chem.** 168: 175-183.

Charton, P. and Armand, P. (2004). X-ray absorption and Raman characterizations of TeO_2–Ga_2O_3 glasses. **Journal of Non-Crystalline Solids.** 333:307–315.

Chen, W., Wang, Z., and Lin, L. (1977). Thermoluminescence of CdS clusters in zeolite-Y. **Journal of Luminescence.** 71: 709-712.

Curie, Daniel. (1963). **Luminescence in Crystal.** New York.

Dr. Saad B. H. Farid (2008). Mixed alkali effect on viscosity of sodium potassium of borate glasses. **Journal of Engineer and Technology, University of Tech, Baghdad, Iraq.** 26:387.

Duffy, J.A. (1996). Redox equilibria in glass. **Journal of Non-crystalline Solids.** 196 : 45-50.

Elvers, A. and Weibmann, R. (2001). ESR spectroscopy-an analytical tool for the glass industry. **Glastechnische Berichte-Glass Science and Technology.** 74: 32-38.

Garcia, J. A., Ramons, A., Munoz, V., and Triboulet, R. (1998). Photoluminescence study of radiative transitions in ZnTe bulk crystals. **Journal of Crystal Growth.** 191: 685-691.

Guha, S., Leppert, V-J., and Risbud, S-H. (1998). Identification of the electronic states of Se^{2-} molecules embedded in borosilicate glasses and Se-based nanometer sized crystals. **Journal of Non-Crystalline Solids.** 240: 43-49.

Halpern, A.M. (2005). Luminescence. **Encyclopedia of Physics.** 1349-1351.

Hayakawa, Y., Fukunaga, K., Tai, Y., Murakami, J., and Nakamura, A. (2006). Ultrafast relaxation dynamics of electrons in Au clusters capped with dodecanethiol molecules. **Journal of Luminescence.** 119-120: 423-427.

Kamimura, H., Sugano, S., and Tanabe, Y. (2005). **Ligand Field Theory and Its Application.** Tokyo: Syokabo [in Japanese].

Khonthon, S., Morimoto, S., Arai, Y., and Ohishi, Y. (2009). Redox equilibrium and NIR luminescence of Bi_2O_3-containing glasses. **Optical Materials.** 31: 1262.

Khonthon, S., Punpai P., Morimoto, S., Arai, Y., Suzuki, T., and Ohishi, Y. (2008). On the near-infrared luminescence from TeO_2 containing borate glasses. **Journal of the Ceramic Society of Japan.** 116: 829-831.

Khonthon, S., Morimoto, S., Arai, Y., and Ohishi, Y. (2007). Luminescence characteristics of Te-and Bi-doped glasses and glass-ceramics. **Journal of the Ceramic Society of Japan.** 115: 259-263.

Khonthon, S., Morimoto, S., and Ohishi, Y. (2006). Absorption and emission spectra of Ni-doped glasses and glass-ceramics in connection with its co-ordination number. **Journal of the Ceramic Society of Japan.** 114: 791-794.

Kishino, M., Tanaka, S., Senda, K., Yamada, Y., and Taguchi, T. (2000). Photoluminescence characterization of MBE-grown $ZnTe_xSe_{1-x}$ epitaxial layers with high Te concentrations. **Journal of Crystal Growth.** 214-215: 220-224.

Konishi, T., et al. (2003). Investigation of glass formation and color properties in the P_2O_5-TeO_2-ZnO system. **Journal of Non-Crystalline Solids.** 324: 58-66.

Lee, C.D., Kim, H.K., Park, H.L. Chung, C.H., and Chang, S.K. (1991). Luminescence from free and self-trapped excitons in $ZnSe_{1-x}Te_x$. **Journal of Luminescence.** 48-49: 116-120.

Lenntech Water. (2008). **Glass** [on-line]. Available: http://www.lenntech.com/ Glass.html

Li, H., Wu, X., and Song, R. (2008). Nd-doped YVO_4 waveguide films prepared by pulsed laser deposition. **Materials Characterization.** 59:1066-1069.

Lindner, G-G., Witke, K., Schlaich, H., and Reinen, D. (1996). Blue-green ultramarine-type zeolites with dimeric tellurium color centers. **Inorganica Chimica Acta.** 252: 39-45.

Mekki, A., Khattak, G.D., and Wenger, L.E. (2006). Structural and magnetic investigations of Fe_2O_3–TeO_2 glasses. **Journal of Non-Crystalline Solids.** 352: 3326-3331.

Miyoshi, T., Towata, K., Matsuki, H., and Matsuo, N. (1997). Luminescence and ESR studies of photodarkening in CdS-doped glasses. **Journal of Luminescence.** 72-74: 368-369.

Murata, T. and Mouri, T. (2007). Matrix effect on absorption and infrared fluorescence properties of Bi ions in oxide glasses. **Journal of Noncrystalline Solids.** 353: 2403-2407.

Ohishi, Y., Mori, A., Yamada, M., Ono, H., Nishida, Y., and Oikawa, K. (1998). Gain characteristics of tellurite-based erbium-doped fiber amplifiers for 1.5 µm broadband amplification. **Optics Letters.** 23: 274-276.

Pal, U., Fernandez, P., and Piqueras, J. (1995). Study of defects in CdTe: Cl by cathodoluminescence microscopy. **Materials Letters.** 23: 227-230.

Park, S. H., Heo, J., and Kim, H. S. (1999).Compositional dependence of the 1.3 µm emission and energy transfer mechanism in Ge-Ga-S glasses doped with Pr^{3+}. **Journal of Non-Crystalline Solids.** 259: 31-38.

Paul, A. (1990). **Chemistry of Glass.** London: Chapman and Hall.

Paul, A. (1975). Mechanism of selenium pink coloration in glass. **Journal of Materials Science.** 10: 415-422.

Perceives, V., Gayen, S.K., and Alfano, R.R. (1988). Laser action in chromiumactivated forsterite for near-infrared excitation: Is Cr4 + the lasing ion. **Applied Physics Letters.** 53: 2590-2592.

Rawson, H. (1980). **Properties and Applications of Glass.** New York: Elsevier Scientific Publishing.

Ren, J., et al. (2007). Ultrabroad infrared luminescence from Bi-doped aluminogermanate glasses. **Solid State communications.** 141: 559-562.

Rp-photonics. (2008). Rare earth doped gain media [On-line]. Available: http://www.rp-photonics.com/rare_earth_doped_gain_media.html.

Sabadel, J.C., Armand, P., Lippens, P.E., Cachau-Herreillat, D., and E. Philippot. (1999). Mössbauer and XANES of TeO_2–BaO–TiO_2 glasses. **Journal of Non-Crystalline Solids.** 244: 143-150.

Sakamoto, T., et al. (1995). 1.4-µm-band gain characteristics of a Tm-Ho-doped ZBLYAN fiber amplifier pumped in the 0.8-µm band. **IEEE Photonics Technology Letters.** 7: 983-985.

Sigel Jr., G.H. (1977). Glass I: Interaction with eletromagnetic radiation. In Tomozawa, M. and Doremus (eds). **Treatise on Materials Science and Technology** (pp. 5-89). New York: R.H. Academic Press.

Sorokina, T.I., Naumov, S., Sorokin, E., Wintner, E., and Shestakov, A.V. (1999). Directly diode-pumped tunable continuous-wave room-temperature Cr^{4+}YAG laser. **Optics Letters**. Vol.24: 1578-1580.

Suzuki, T., Murugan, G.S., and Ohishi, Y. (2005). Spectroscopic properties of a novel near-infrared tunable laser material Ni: MgGa2O4. **Journal of Luminescence.** 113: 265-270.

Trigg, George L. (ed.). (2006). Optical networks. **The optics Encyclopedia** (Vol.4).

Varshneya, A.K. (1994). Glass Composition and Structure. **Fundamentals of Inorganic Glasses.** Academic press.

Vreugdenlik, A-J., Pilatzke, K-K., and Parnis J-M. (2006). Characterization of laser ablated gold nanoparticles encapsulated in epoxy amine crosslinked sol-gel materials. **Journal of Non-Crystalline Solids.** 352: 3879-3886.

Wells, A. F. (1975). Sulphur, Selenium, and Tellurium. **Structural Inorganic Chemistry** (pp. 570-604). Oxford: Wells, A. F. Clarendon Press.

Wikipedia. (2008). **Optical amplifier** [On-line]. Available: http://en.wikipedia.org/ wiki/ Erbium_doped_fiber_amplifiers.html

Wikipedia. (2009). Soda-lime glass [on-line]. Available: http://en.wikipedia.org/wiki/ Soda-lime glass.html

APPENDIX A

JCPDS-XRD PATTERNS OF TELLURIUM

Table A1 JCPDS 00-003-0506 of tellurium

Pattern: 00-003-0506		*Radiation=* 1.540598			*Quality:* Deleted

		2th	*i*	*h*	*k*	*l*
		23.454	40	1	0	0
Te		27.947	100	1	0	1
		38.610	80	1	0	2
		40.797	80	1	1	0
Tellurium		43.917	60	1	1	1
		46.284	60	0	0	3
		50.079	80	2	0	1
		51.596	20	1	1	2
Lattice: Hexagonal	*Mol. Weight=* 127.60	57.168	60	2	0	2
		63.204	60	1	1	3
S.G. : (0)	*Volume [CD]=* 101.13	64.179	40	2	1	0
		66.229	60	2	1	1
a = 4.44500	*Dx=* 2.095	67.861	60	1	0	4
		72.675	40	2	1	2
		76.084	20	3	0	1
c = 5.91000		82.352	60	2	1	3
		89.934	10	2	2	1
		94.381	20	3	1	1
		95.577	20	2	2	2
		100.761	20			
		125.619	10	3	1	4

Deleted and rejected by: Deleted by NBS card.
Color: Dark gray
Data collection flag: Ambient.

Inst. of phys. at College, Cardiff, Wales

Radiation : CuKa	*Filter :* Beta
Lambda : 1.54180	*d-sp :* Not given
SS/FOM : F20= 2(0.2110,53)	

APPENDIX B

CALCULATION OF OPTICAL BASICITY

Calculation of Optical Basicity

Duffy and Ingram defined the theoretical optical basicity (Λ) as follows:

$$\Lambda = \Sigma(xi/fi) \tag{B1}$$

where, xi is the equivalent cationic fraction and f_i is the basicity moderating parameter for the constituent cation i, respectively (Key to Metals, www, 2008).

Table B1 Optical basicity, Λ for some oxides

Oxides	Λ/Duffy
P_2O_5	0.33
B_2O_3	0.42
SiO_2	0.48
Al_2O_3	0.60
MgO	0.78*
CaO	1.00
SrO	1.10*
BaO	1.15*
K_2O	1.40*
Na_2O	1.15*
FeO	1.00*

Remark: * Reddy, 1999.

Optical basicity, Λ, of glass composition was calculated as follow:

$\Lambda = X_A\Lambda(A) + X_B\Lambda(B) + \ldots\ldots$

X_A, X_B,… are the molar proportions contributed by the constituent oxides, A, B,… to the total oxide(-II) content of the glass (that is, the equivalent fractions) and $\Lambda(A)$, $\Lambda(B)$,… are the optical basicity values of these individual oxides (Duffy,1996).

Calculation of Λ for borate glasses

A glass of composition: $90[10Al_2O_3 \, (80-X)B_2O_3 \cdot 10ZnO \cdot X \, K_2O]$

X-0; $10Al_2O_3 \cdot 80B_2O_3 \cdot 10ZnO$

$(9Al_2O_3 \cdot 72B_2O_3 \cdot 9ZnO)$

The total oxygen $= (0.09\times3) + (0.72\times3) + 0.09$

$= 0.27+2.16+0.09$

$= 2.52$

$$\Lambda = \frac{(0.72\times3)\,(0.42)}{2.52} + \frac{(0.09\times3)\,(0.6)}{2.52} + \frac{(0.09)\,(0.95)}{2.52}$$

$= 0.36+0.064+0.0339$

$= 0.4579 \approx 0.46$

X-10; $10Al_2O_3 \cdot 70B_2O_3 \cdot 10ZnO \cdot 10K_2O$

$(9Al_2O_3 \cdot 63B_2O_3 \cdot 9ZnO \cdot 9K_2O)$
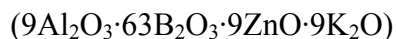
The total oxygen $= (0.09\times3) + (0.63\times3) + 0.09 + 0.09$

$= 0.27+1.89+0.09+0.09$

$= 2.34$

$$\Lambda = \frac{(0.63\times3)\,(0.42)}{2.34} + \frac{(0.09\times3)\,(0.6)}{2.34} + \frac{(0.09)\,(0.95)}{2.34} + \frac{(0.09)\,(1.4)}{2.34}$$

$= 0.3392+0.0692+0.0365+0.0538$

$= 0.4987 \approx 0.50$

X-20; $10Al_2O_3 \cdot 60B_2O_3 \cdot 10ZnO \cdot 20K_2O$

$(9Al_2O_3 \cdot 54B_2O_3 \cdot 9ZnO \cdot 18K_2O)$

The total oxygen $= (0.09 \times 3) + (0.54 \times 3) + 0.09 + 0.18$

$= 0.27+1.62+0.09+0.18$

$= 2.16$

$$\Lambda = \frac{(0.54 \times 3)(0.42)}{2.16} + \frac{(0.09 \times 3)(0.6)}{2.16} + \frac{(0.09)(0.95)}{2.16} + \frac{(0.18)(1.4)}{2.16}$$

$= 0.315+0.075+0.0396+0.1167$

$= 0.5463 \approx 0.55$

X-30; $10Al_2O_3 \cdot 50B_2O_3 \cdot 10ZnO \cdot 30K_2O$

$(9Al_2O_3 \cdot 45B_2O_3 \cdot 9ZnO \cdot 27K_2O)$

The total oxygen $= (0.09 \times 3) + (0.45 \times 3) + 0.09 + 0.27$

$= 0.27+1.35+0.09+0.27$

$= 1.98$

$$\Lambda = \frac{(0.45 \times 3)(0.42)}{1.98} + \frac{(0.09 \times 3)(0.6)}{1.98} + \frac{(0.09)(0.95)}{1.98} + \frac{(0.27)(1.4)}{1.98}$$

$= 0.2864+0.0818+0.0432+0.1909$

$= 0.6023 \approx 0.60$

Borate compositions: X-0; Λ=0.46

X-10; Λ=0.50

X-20; Λ=0.55

X-30; Λ=0.6

APPENDIX C

DETERMINATION OF GLASS TRANSITION

TEMPERATURE (Tg) AND DILATOMETRIC

SOFTENING POINT (Td)

Determination of glass transition temperature (Tg) and dilatometric softening point (Td)

Glass transition temperature (Tg) and dilatometric softening point (Td) can be determined by Differential thermal analysis (DTA) and dilatometer. In DTA, the material under study and an inert reference are made to undergo identical thermal cycles, while recording any temperature difference between sample and reference. This differential temperature is then plotted against time, or against temperature (DTA curve or thermogram). Changes in the sample, either exothermic or endothermic, can be detected relative to the inert reference. Thus, a DTA curve provides data on the transformations that have occurred, such as glass transitions, crystallization, melting and sublimation (Wikipedia, www, 2010). DTA curve which exhibit a slope change that attributed to the glass transition (Branda et al., 1984). Traditionally, the dilatometric transition temperature (Tg) is determined from the $\Delta L/L_o$ curve as the point of intersection of the tangents below and above the slope change as shown in Figure C2 (Wikipedia, www, 2010).
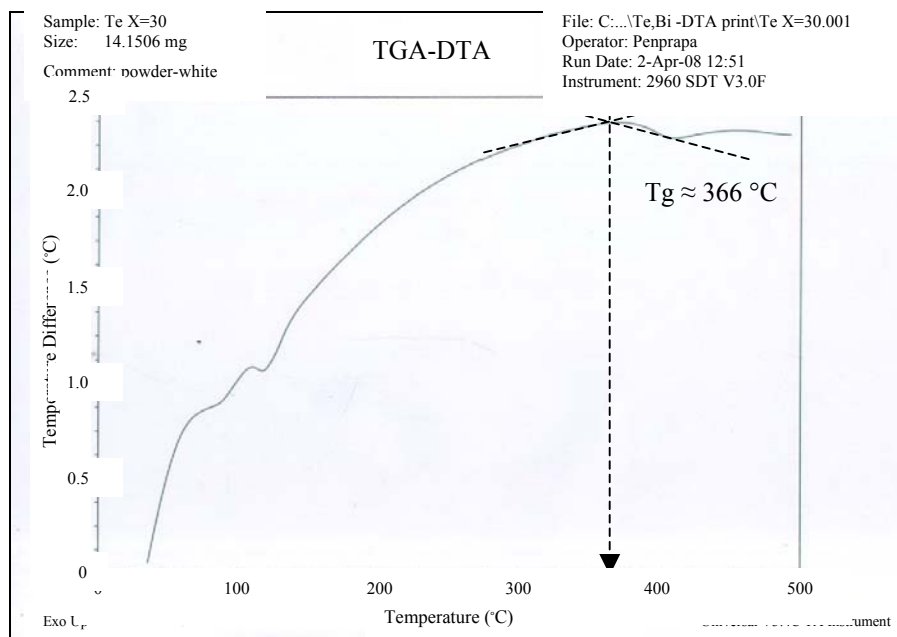
Figure C1 Shows an example to determined of glass transition temperature (Tg)

of the TeO_2-containing borate glass by the DTA curve.
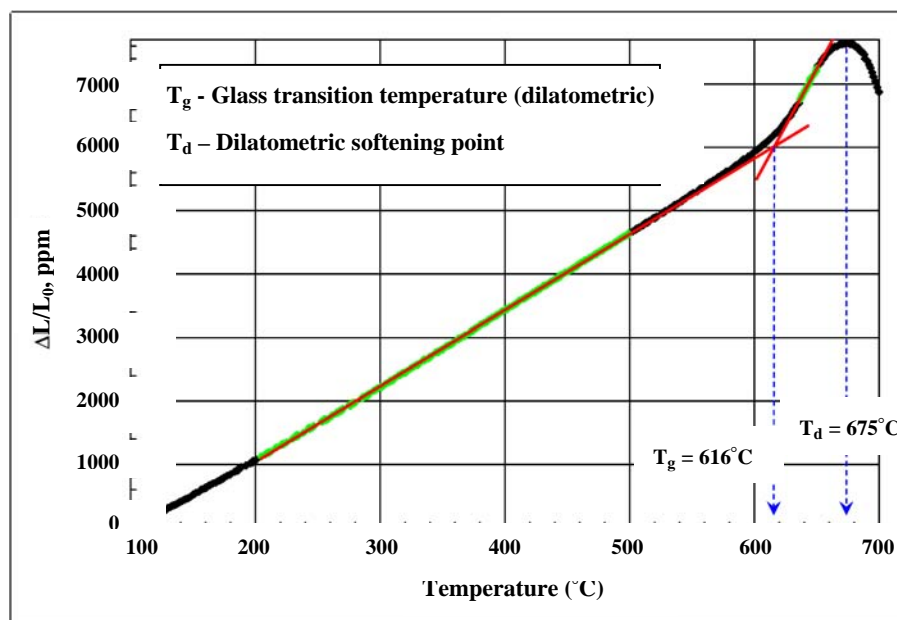
Figure C2 Determination of glass transition temperature (Tg) and dilatometric

softening point (Td) by dilatometry (Glassproperties, www, 2010)

APPENDIX D

LIST OF PUBLICATIONS

LIST OF PUBLICATIONS

I. Papers

Sasithorn Khonthon, Penprapa Punpai, Shigeki Morimoto, Yusuke Arai, Takenobu Suzuki, and Yasutake Ohishi. (2008). On the near-infrared luminescence from TeO_2 containing borate glasses. **Journal of the Ceramic Society of Japan**. 116: 829-831.

Penprapa Punpai, Shigeki Morimoto, Sasithorn Khonthon, Yusuke Aria, Takenobu Suzuki, and Yasutake Ohishi.(2008). Effect of carbon addition and TeO_2 concentration on the NIR luminescent characteristics of TeO_2-doped soda-lime-silicate glasses. **Journal of Non-Crystalline Solids**. 354:5529-5532.

II. Presentations

Sasithorn Khonthon, Penprapa Punpai, Shigeki Morimoto*, Yusuke Arai, and Yasutake Ohishi. (2007). Near-infrared luminescent center of Te-doped glasses. **The 48th Symposium on Glasses and Photonics Materials, Glass Division of The Ceramic Society of Japan.** Proceeding P06, 29-30/Nov./2007, Toyohashi, Japan [Poster presentation]

Penprapa Punpai*, Shigeki Morimoto, Sasithorn Khonthon, Yusuke Arai, and Yasutake Ohishi. (2008). Near-infrared luminescent center of Te-doped sodalime-silicate glasses. **The 3rd Siam Physics Congress 2008 (SPC2008)**.Proceedings A-5, 20-22/March/2008, Khao Yai, Thailand. [Oral presentation]

Effect of carbon addition and TeO$_2$ concentration on NIR luminescent characteristics of TeO$_2$-doped soda-lime–silicate glasses

Penprapa Punpai [a,*], Shigeki Morimoto [a], Sasithorn Khonthon [a], Yusuke Arai [b], Takenobu Suzuki [b], Yasutake Ohishi [b]

[a] School of Ceramic Engineering, Institute of Engineering, Suranaree University of Technology, 111, University Avenue, Muang District, Nakhon Ratchasima 30000, Thailand
[b] Research Center for Advanced Photon Technology, Toyota Technological Institute, 2-12-1, Hisakata, Tempaku-ku, Nagoya-shi 468-8511, Japan

ARTICLE INFO

ABSTRACT

The effects of carbon addition and TeO$_2$ concentration on the near-infrared (NIR) luminescent characteristics of Te-doped soda-lime–silicate glasses are investigated. Three absorption bands were detected in all glasses at around 330–380 nm, ~430 nm and ~630 nm, respectively. The last absorption band (~630 nm) has been ascribed to $^2\Pi g \rightarrow ^2\Pi u$ transition of Te$_2^-$. The broad NIR luminescence centered at 1200 nm was detected under the excitation of 974 nm laser diode except for glasses of lower carbon addition. The NIR luminescence was found to be strongly affected by melting atmosphere and TeO$_2$ concentration. It is considered that the absorption band, ~630 nm, is related strongly to the NIR luminescence of Te-doped soda-lime–silicate glasses. Consequently, it is suggested that the origin of NIR luminescence detected in Te-doped soda-lime–silicate glasses is likely to be caused by Te$_2^-$.

© 2008 Elsevier B.V. All rights reserved.

1. Introduction

Tellurite glasses (high TeO$_2$-containing glasses) have received much attention as promising candidates for new glass because of their special properties [1–5], high nonlinear refractive indices [6], large nonlinear optical sensibility [6–9], relatively low phonon energy in the blue [10] and green band emission [11], wide transmission window and good stability and durability [3,4,12,13]. In addition these glasses are well known to be good hosts for some rare earth and heavy metal ions with small multi-phonon decay rate [6,14,15], and they are potential materials for up-conversion lasers [16,17], optical fiber amplifiers [18], such as tellurite-base Er-doped fiber amplifier [19], nonlinear optical devices, such as optical switching [6], optical memory, etc. [6].

However, high TeO$_2$-containing glasses often show the coloration, pale green to brilliant purple, depending on glass compositions and melting conditions [20,21]. Few research [20,22] has been reported on the coloration and color centers of TeO$_2$-containing glasses, their coloration change from pale green to brilliant purple depending on melting conditions and glass compositions. The color center of pale green TeO$_2$-containing glasses is clusters of Te:Te$_2$ and Te$_2^-$ [22], that of brilliant purple TeO$_2$ glasses is Te-metallic colloids [20].

Recently, the authors have found near-infrared (NIR) luminescence centered at 1250 nm with 250 nm of half width from pale green and purple TeO$_2$-containing glasses for the first time to our knowledge [23–25], and we concluded that the NIR luminescent center might be Te$_2$ and Te$_2^-$. In this paper, the effects of carbon addition and TeO$_2$ concentration on NIR luminescent characteristics of TeO$_2$-doped soda-lime–silicate glasses are investigated and compared with previous work [23].

2. Experimental

2.1. Sample preparation

Two series of glasses were prepared. In series (I) glasses, compositions was $72SiO_2 \cdot 2Al_2O_3 \cdot 4MgO \cdot 8CaO \cdot 13Na_2O \cdot 1K_2O \cdot 1TeO_2 \cdot Xcarbon$ (X = 0–1, wt%). Series (II) glasses, compositions was $72SiO_2 \cdot 2Al_2O_3 \cdot 4MgO \cdot 8CaO \cdot 13Na_2O \cdot 1K_2O \cdot XTeO_2 \cdot 0.3$carbon (X = 0.2–2, wt%).

High purity silica sand, alumina and reagent grade chemicals of MgO, $CaCO_3$, Na_2CO_3, K_2CO_3, TeO_2 and carbon were used as raw materials. Batches corresponding to 25 g of glass were mixed thoroughly and melted in 50 cc alumina crucible at 1450 °C for 1 h in an electric furnace in air. After melting they were poured onto iron plate and pressed by another iron plate. Then they were annealed at 600 °C for 30 min and cooled slowly in the furnace.

The glasses were cut and polished optically into about 2 mm in thickness for optical measurements. Hereafter, these glasses are referred to as C-0, C-0.1, C-0.2, C-0.3, C-0.5, C-1.0 and Te-0.2, Te-0.5, Te-0.7, Te-1.0, Te-2.0, respectively.

2.2. Absorption and luminescence measurement

The absorption spectra were measured with Cary 1E ultraviolet-visible (UV–Vis) spectrometer in the range of 300 nm to 800 nm at room temperature.

The luminescence spectra in the NIR region (1000–1700 nm) were measured under the excitation of 974 nm laser diode at room temperature. Emission from the sample were dispersed by a single monochromator (blaze, 1.0 nm; grating, 600 grooves/mm; resolution, 3 nm) and detected by an InGaAs photodiode.

3. Result and discussion

3.1. Absorption spectra

The appearances of glasses in series I change from colorless (C-0) to dark green–black (C-1.0) with increase in the amount of carbon addition. In series II, color of glasses change from green (Te-0.2) to pale green (Te-2.0) with increase in TeO_2 concentration. Fig. 1 shows absorption spectra of TeO_2-doped soda-lime–silicate glasses of series I and II glasses. Appearances and absorption bands of glasses are summarized in Table 1.

Three absorption bands can be observed in all glasses, 330–380 nm, ~430 nm, ~630 nm, respectively. In series I glasses, weak absorption bands can be detected even in C-0 glass, the absorbance increases with increase in the amount of carbon, and the absor-
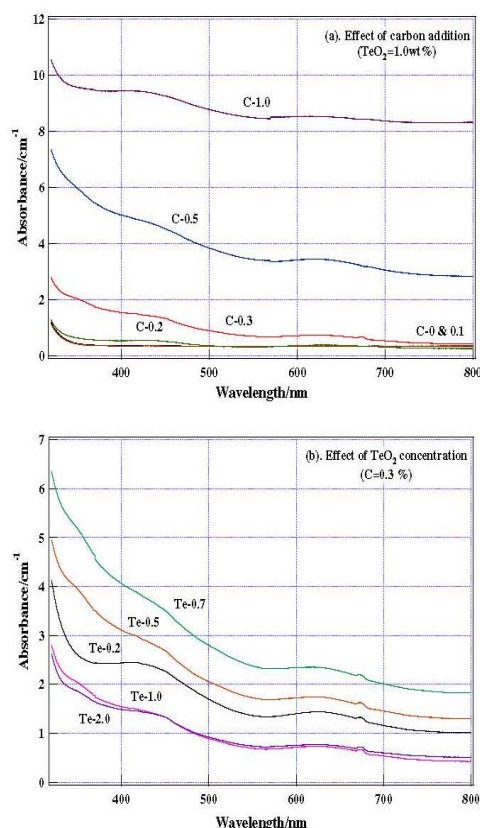
Fig. 1. Absorption spectra of TeO_2-doped glasses. (a) Effect of carbon addition (TeO_2 = 1.0 wt%).(b)Effect of TeO_2 concentration (Carbon = 0.3 wt%).

bance is very high in whole wavelength region in C-0.5 and C-1.0 glasses.

On the other hand, the absorbance of series II glasses increases with increase in the amount of TeO_2 (0.2–1.0 wt%) and decreases again. However, the absorption band owing to Te-metallic colloids (~530 nm) cannot be observed in all glasses discussed here.

The assignment of these absorption bands has been already known that absorption band (I) is due to exciton transition, band (II) $^3\Sigma g^- \rightarrow {}^3\Sigma u^-$ transition of Te_2, band (III) Te metallic colloids and band (IV) $^2\Pi g \rightarrow {}^2\Pi u$ transition of Te_2^- [20,21], respectively.

Table 1
Melting conditions, appearance and absorption bands of glasses studied

No.	Melting condition (°C min)	Appearance	Absorption bands/nm			
			I	II	III	IV
C-0	1450-60	Colorless	~380[a]	432	–	638[a]
C-0.1	1450-60	Pale green	~380[a]	432	–	638[a]
C-0.2	1450-60	Green	377[a]	432	–	638[a]
C-0.3	1450-60	Green	327	435	–	633
C-0.5	1450-60	Dark green	355	436	–	638
C-1.0	1450-60	Dark green-black	375	438	–	634
Te-0.2	1450-60	Green	367	437	–	635
Te-0.5	1450-60	Green, partly brownish green	344	432	–	633
Te-0.7	1450-60	Green, partly brownish green	349	435	–	634
Te-1.0	1450-60	Green	327	435	–	633
Te-2.0	1450-60	Green	331	436	–	633
Te-1200[b]	1200-20	Reddish orange	370	430	530	–

[a] Very weak.
[b] $63B_2O_3 \cdot 9Al_2O_3 \cdot 9ZnO \cdot 9K_2O \cdot 10TeO_2$ (mol%) melted in alumina crucible [25].
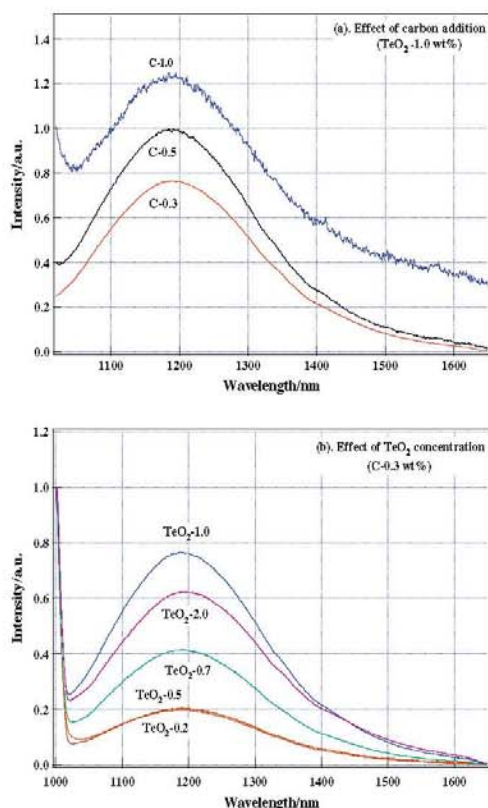
Fig. 2. NIR luminescence spectra of TeO₂-doped soda-lime-silicate glasses. (a) Effect of carbon addition (TeO₂ = 1.0 wt%). (b) Effect of TeO₂ concentration (Carbon = 0.3 wt%).

Fig. 3. NIR luminescence intensity of TeO₂-doped soda-lime-silicate glasses. (a) Effect of carbon addition (TeO₂ = 1.0 wt%). (b) Effect of TeO₂ concentration (Carbon = 0.3 wt%).

For comparison with Te-doped soda-lime-silicate glasses, the absorption bands of Te-containing borate glasses are also shown in Table 1. The band III was observed but the band IV could not be detected in borate glasses.

3.2. NIR luminescence

Fig. 2 shows the NIR luminescence spectra of glasses under the excitation of 974 nm laser diode at room temperature. In these glasses, the strong and broad emission band can be observed at around 1200 nm except for glasses of lower carbon addition (C-0, C-0.1 and C-0.2 glasses). In series I glasses, the luminescent intensity increases with increase in the amount of carbon (Fig. 3(a)). On the contrary, the luminescent intensity of series II glasses increases with increase in TeO₂ concentration and reaches to the maximum at TeO₂ = 1.0 wt% and decrease slightly again at TeO₂ = 2.0 wt% (Fig. 3(b)). Thus the intensity of NIR luminescence was strongly affected by melting atmosphere and TeO₂ concentration.

The authors have investigated color generation and NIR luminescence characteristics of Te-containing borate glasses melted under various conditions [25]. Though the coloration of glasses changed depending on melting conditions and glass compositions, the green-colored glass could not be obtained. In these glasses, three absorption bands were observed, ~370 nm, ~430 nm and ~530 nm, however, the band at around ~630 nm could not be detected. One example of borate glasses is shown in Table 1. As mentioned previously, the band at ~530 nm is due to Te-metallic

colloids [20]. These borate glasses did not exhibit any NIR luminescence under the excitation of 974 nm laser diode.

Lindner et al. [22] have reported that two luminescence bands could be observed at 562 nm and 862 nm under the excitation of 457 nm, and they concluded that the former band was ascribed to $^3\Sigma u^- \rightarrow {^3}\Sigma g^-$ transition of Te₂ and the latter was due to $^2\Pi u \rightarrow {^2}\Pi g$ of Te₂⁻. However, they did not observe the NIR luminescence (>1000 nm). On the contrary, band IV (~630 nm) was observed in all Te-doped soda-lime-silicate glasses discussed here, and the NIR luminescence was detected under the excitation of 974 nm except for glasses of low carbon addition (C-0, C-0.1 and C-0.2). All borate glasses without absorption band IV did not show any NIR luminescence. Therefore, it is considered that the color center of band IV (~630 nm) is strongly related to NIR luminescence.

Consequently, it is suggested that the NIR luminescent center of Te-doped soda-lime-silicate glasses is likely to be caused by Te₂⁻.

4. Conclusion

The effects of carbon addition and TeO₂ concentration on the NIR luminescent characteristics of Te-doped soda-lime-silicate glasses are investigated. All glasses appear to be green in color. The color becomes to be deeper with increase in the amount of carbon addition at constant TeO₂ concentration. And also the color changes from green to brownish green and again pale green with increase in TeO₂ concentration at constant carbon amount. Three absorption bands were detected in all glasses, 330–380 nm,

~430 nm and ~630 nm, respectively. The last absorption band (~630 nm) has been ascribed to $^2\Pi g \rightarrow {}^2\Pi u$ transition of Te_2^-.

The broad NIR luminescence centered at around 1200 nm was detected under the excitation of 974 nm laser diode except for glasses of lower carbon addition. The NIR luminescence was found to be strongly affected by melting atmosphere and TeO_2 concentration. It is considered that the absorption band (~630 nm), is related strongly to NIR luminescence of Te-doped soda-lime–silicate glasses.

Consequently, it is suggested that the origin of NIR luminescence detected in Te-doped soda-lime–silicate glasses is likely to be caused by Te_2^- center.

Acknowledgement

References

[1] M. Yamada, A. Mori, K. Kobayashi, H. Ono, T. Kanamori, K. Oikawa, Y. Nishida, Y. Ohishi, IEEE Photon. Technol. Lett. 10 (1998) 1244.
[2] Y. Mizuno, New Glass 6 (3) (1991) 258.
[3] G.S. Murugan, Y. Ohishi, J. Non-Cryst. Solids 341 (2004) 86.
[4] G.S. Murugan, Y. Ohishi, J. Non-Cryst. Solids 351 (2005) 364.
[5] M. Zambelli, A. Speghini, G. Ingletto, C. Locatelli, M. Bettinelli, F. Vetrone, J.C. Boyer, J.A. Capobianco, Opt. Mater. 25 (2004) 215.
[6] J. Li, Z. Sun, X. Zhu, H. Zeng, Z. Xu, Z. Wang, J. Lin, W. Huang, R.S. Armstrong, P.A. Jay, Opt. Lett. 25 (1998) 401.
[7] K. Tanaka, A. Narazaki, K. Hirao, Opt. Lett. 25 (2000) 251.
[8] A. Narazaki, K. Tanaka, K. Hirao, N. Soga, J. Appl. Phys. 85 (1999) 2046.
[9] G.V. Prakash, D.N. Rao, A.K. Bhatnagar, Solid State Commun. 119 (2001) 39.
[10] H.D. Lee, H.K. Kim, H.L. Park, C.H. Chung, S.K. Chang, J. Lumines. 48&49 (1991) 116.
[11] M. Kishino, S. Tanaka, K. Senda, Y. Yamada, T. Taguchi, J. Cryst. Growth 214&215 (2000) 220.
[12] Y. Ohishi, A. Mori, M. Tamada, H. Ono, Y. Nishida, K. Oikawa, Opt. Lett. 23 (1998) 274.
[13] A. Mori, T. Sakamoto, K. Kobayashi, K. Shikano, K. Oikawa, K. Oshino, T. Takamori, Y. Ohishi, M. Shimizu, IEEE J. Lightwave Technol. LT-20 (1957) 332.
[14] J.S. Wang, E.M. Vogel, E. Snitzer, Opt. Mater. 3 (1994) 187.
[15] V.P. Gapontsev, S.M. Matistsi, A.A. Isineev, V.B. Kravchenko, Opt. Laser Technol. 14 (1989) 189.
[16] T. Tamaoka, S. Tanabe, S. Ohara, H. Hayashi, N. Sugimoto, J. Alloys Comp. 408–412 (2006) 848.
[17] S. Xu, D. Fang, Z. Zhang, Z. Jiang, Spectrochim. Acta A Mol. Biomol. Spectrosc. 62 (2005) 690.
[18] F. Vetrone, J.C. Boyer, J.A. Capobianco, A. Speghini, M. Bettinelli, Appl. Phys. Lett. 80 (2002) 1752.
[19] Y. Ohishi, A. Mori, H. Yamada, H. Ono, Y. Nishida, K. Oikawa, Opt. Lett. 23 (1998) 167.
[20] S. Konishi, T. Hondo, T. Araki, K. Nishio, T. Tsuchiya, Y. Matsumoto, S. Suehara, S. Todoroki, S. Inoue, J. Non-Cryst. Solids 324 (2003) 58.
[21] Y. Hasegawa, S. Sakamoto, Glastech. Ber. 30 (1957) 332.
[22] G.-G. Lindner, K. Witke, H. Schlaich, D. Reinen, Inorg. Chim. Acta 252 (1996) 39.
[23] S. Khonthon, S. Morimoto, Y. Arai, Y. Ohishi, J. Ceram. Soc. Jpn. 115 (2007) 259.
[24] Y. Arai, T. Suzuki, Y. Ohishi, S. Morimoto, XXIst International Congress on Glass, in: Proceedings M6, Strausbourg, France, 1–6 July 2007.
[25] S. Khonthon, P. Punpai, S. Morimoto, Y. Arai, Y. Ohishi, J. Ceram. Soc. Japan, 116 (2008) 829.

On the near-infrared luminescence from TeO₂ containing borate glasses

Sasithorn KHONTHON, Penprapa PUNPAI, Shigeki MORIMOTO, Yusuke ARAI,⁺ Takenobu SUZUKI⁺ and Yasutake OHISHI⁺

School of Ceramic Engineering, Institute of Engineering, Suranaree University of Technology, 111 University Avenue, Muang District, Nakhon Ratchasima 30000, Thailand
⁺Research Center for Advanced Photon Technology, Toyota Technological Institute, 2–12–1, Hisakata, Tempaku, Nagoya 468–8511, Japan

The effects of melting temperature and glass composition on the Near-infrared (NIR) luminescent characteristics of Te-containing borate glasses are investigated and compared with previous works. Three absorption bands are detected at around ~370 nm, ~430 nm and ~530 nm, however, the absorption band at around ~600 nm could not be detected in all borate glasses. And no NIR luminescence was observed under the excitation of a 974 nm laser diode. The NIR luminescence was observed in Te-green and Te-purple glasses, which showed the absorption band at around ~600 nm. This absorption band was ascribed to $^2\Pi g \rightarrow {}^2\Pi u$ transition of Te_2^-. Consequently, it is suggested that the origin of NIR luminescence of Te-containing green and purple glass is likely to be caused by Te_2^- center.
©2008 The Ceramic Society of Japan. All rights reserved.

Key-words : Tellurium, Borate glass, Color center, NIR luminescence, Clusters

1. Introduction

Among non-silicate glasses, such as heavy metal oxide and non-oxide glasses, high TeO₂ containing glasses are promising candidate materials for photonics applications, unifying the following features (1) wide transmission window, (2) good glass stability and durability and (3) high refractive index, better non-linear optical properties and relatively low phonon energy. Broad band erbium doped fiber amplifiers (EDFAs) have been demonstrated using TeO₂-based fibers as erbium hosts.[1],[2]

However, high TeO₂ containing glasses often show coloration, pale green, brilliant purple to dark red, depending on glass composition and melting conditions.[3],[4] The color centers of these glasses have already been reported.[4],[5] According to their reports, the color centers of pale green glasses are clusters of Te_2 and Te_2^- species[5] and those of brilliant purple glasses are Te metallic colloids.[4]

Recently, the authors have found near-infrared (NIR) luminescence centered at 1250 nm with 250 nm of half width from pale green and purple TeO₂-containing glasses for the first time to our knowledge.[6],[7] We concluded that NIR luminescent centers might be Te_2 or Te_2^- species. Thus, the valence state of Te may change depending on glass composition and melting conditions, which produce color center and luminescent center in the glasses. In this study, the effects of melting temperature and glass compositions on the NIR luminescent characteristics of Te-containing borate glasses are investigated and compared with previous works.[6],[7]

2. Experimental

2.1 Sample preparation

Two series of glasses were prepared. Glasses of Series I are the composition of 62B₂O₃·9Al₂O₃·9ZnO·9K₂O·10TeO₂ (mol%), those of Series II are 90[(80–X)B₂O₃·10Al₂O₃·10ZnO·XK₂O]·10TeO₂ (mol%, X = 0, 10, 20 and 30). Reagent grade chemicals of H₃BO₃, Al₂O₃, ZnO, K₂CO₃ and TeO2 were used as raw materials. Batches corresponding to 25 g of glass were mixed thoroughly and melted in 50 cc alumina crucibles under various conditions (850°–1300°C for 15–60 min) in an electric furnace in air for Series I glasses. Glasses of Series II were melted in 50 cc alumina crucibles at 1200°C for 20 min in an electric furnace in air. After melting they were poured onto iron plate and pressed by another iron plate. Then, they were annealed at 450°C for 30 min and cooled slowly to room temperature in the furnace. All glasses were polished optically into about 1.5–2.0 mm in thickness for optical measurement. Hereafter, these glasses are referred to as Te-850, Te-1000, Te-1100, Te-1200, Te-1300, X = 0, X = 10, X = 20 and X = 30, respectively.

2.2 Optical measurement

The absorption spectra (300–800 nm) were measured using a Cary 1E ultraviolet-visible (UV-VIS) spectrometer at room temperature.

The NIR luminescence spectra (1000–1700 nm) were measured under the excitation of a 974 nm laser diode at room temperature. The optical setup for NIR luminescence measurement is shown in **Fig. 1**. Emission from the samples was dispersed by a single monochromator (blaze, 1.0 mm; grating, 600 grooves/mm; resolution 3 nm) and detected by InGaAs photodiode.

3. Results and discussion

3.1 Appearance and absorption spectra

The colors of Series I glasses change from colorless (Te-850) to brown (Te-1300) with increase in melting temperature. In glasses of Series II, color changes from reddish orange (X = 10) to colorless (X = 30) with increase in X (increasing amount of
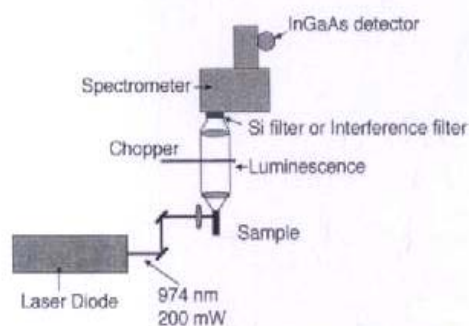
Fig. 1.   Optical setup for NIR luminescence measurement.

K_2O). However, $X = 0$ glass revealed phase separation during casting. The melting conditions and appearance of these glasses are summarized in Table 1.

Figure 2 shows the absorption spectra of Te-containing borate glasses. The absorption spectra were analyzed and separated into three bands using peak fitting with Gaussian distribution. The results are shown in Table 1. Basically, three absorption bands can be observed, ~370 nm (Band I), ~430 nm (Band II) and ~530 nm (Band III), respectively. The assignment of these absorption bands are already known that Band I is the exciton transition, Band II $^3\Sigma g^- \rightarrow ^1\Sigma u^-$ transition of Te_2 and Band III Te metallic colloids.[4),5)] In Series I glasses, the UV absorption increases with an increase in melting temperature. It seems that the melting temperature affects the change in valence of Te. According to redox equilibrium, the higher melting temperature provides a lower valence state of metal ions, and hence the increase in UV absorption might be due to the Te species of a lower valence state.

However, these spectral patterns are different from those reported previously (ZTP, Te-SL and Te-Spinel in Table 1).[6)] The former three absorption bands are the same, but Band IV cannot be detected in all borate glasses discussed in this study. The assignment of Band IV has already been done and is ascribed to $^2\Pi g \rightarrow ^2\Pi u$ transition of Te_2^-.[5)] It is considered that the color center of Te_2^- is lacking in all borate glasses from these results. Lindner et al.[5)] reported that the absorption band due to Te_2^- appeared at 606 nm in Te-doped blue and green sodalite crystal. This position is nearly the same as those in ZTP, Te-SL and Te-Spinel glasses. Thus, the absorption band due to Te_2^- center appeared at around 600 nm in many host materials. If Te_2^- centers are present in borate glasses, the absorption band should appear at around 600 nm. However, this band could not be detected in all borate glasses, and therefore, it is concluded that Te_2^- center is lacking or of a very low concentration in borate glasses.

Te_3 or Te_2 species may be formed during reduction process of TeO_2 to metallic colloids (Te)n in glasses and they gather together and precipitate Te metallic colloids.[4)] Zinc tellurium phosphate glass (ZTP) appeared to be brilliant purple and many small particles were observed by scanning electron microscope (SEM) observation in this glass.[5)] These particles were confirmed to be Te-metallic colloids and the strong absorption at around 537 nm was derived from the surface plasmon resonance absorption of Te-metallic colloids.[4)] This glass contained the same amount of TeO_2 (10 mol%) as that in borate glasses and was melted at nearly the same temperature (1200°C-2 h). This indicates that ZTP glass was prepared under higher reducing condition than borate glasses. According to Duffy's optical basicity concept,[8)] Λ values for both glasses were calculated without TeO_2: ZTP: 0.43 and $X = 0$: 0.46, $X = 10$: 0.50, $X = 20$: 0.55 and $X = 30$, respectively. The Λ value of ZTP is smaller than those f borate glasses. The smaller Λ value provides higher reducing condition, and therefore, a large amount of Te metallic colloids (Te)n was formed in ZTP glass compared with borate glasses. This tendency can be clearly seen in Series II glasses. Thus, the reduction process did not proceed enough in borate glasses and the amount of Te_2 or Te_2^- species seems to be very low. This implies the lacking or very weak absorption of Band IV in borate glasses.

3.2   NIR luminescence

No NIR luminescence can be detected in all borate glasses under the excitation of 974 nm laser diode at room temperature.

Table 1.   Melting Conditions, Appearances and Absorption Bands of Te-containing Glasses

Glass No.	Melting conditions °C-min.	Appearance	Absorption bands/nm			
			I	I	III	IV
Te-850	850-60	Colorless	–	–	–	–
Te-1000	1000-20	Pale orange	370	430**	530**	
Te-1100	1100-20	Orange brown	370	430**	530**	
Te-1200	1200-20	Reddish orange	370	430**	530	
Te-1300	1300-15	Reddish brown	370	430**	530	
X = 0	1200-20	Phase separation	–	–	–	–
X = 10	1200-20	Reddish orange	370	430**	530**	
X = 20	1200-20	Pale orange	370	430**	530**	
X = 30	1200-20	Colorless	–	–	–	–
ZTP*	1200-60	Brilliant purple	375	417	537	600
Te-SL*	1450-60	Pale green	374	444	526**	625
Te-Spinel*	1600-60	Brownish pink	–	420 488**	556	599

*: Reference 6), **: very weak.
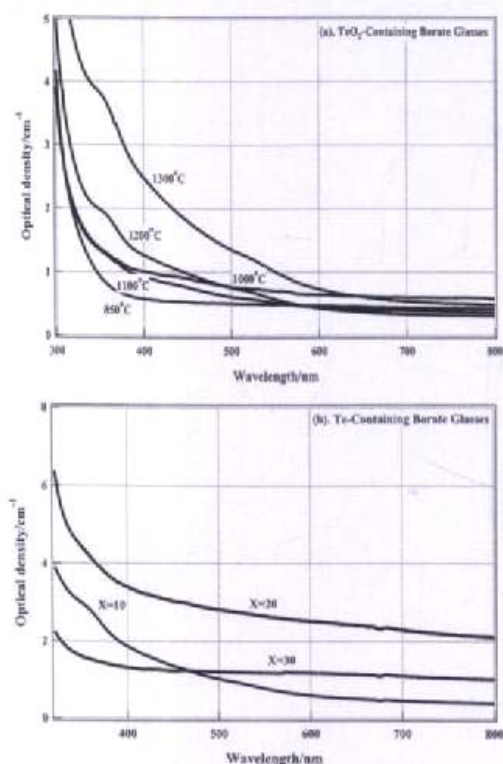
Fig. 2. Absorption spectra of Te-containing borate glasses. (a) Effect of melting temperature, (b) Effect of glass composition.
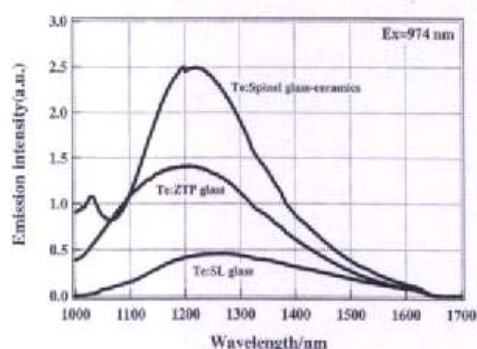
Fig. 3. NIR luminescence spectra of Te-containing glasses and glass-ceramics.[6]

However, as reported previously,[6,7] ZTP, Te-SL and Te-Spinel glasses and glass-ceramics exhibited NIR luminescence centered at around 1200–1250 nm (**Fig. 3**).

In Table 1, the color center of borate glasses is different from those of ZTP, Te-SL and Te-Spinel glass and glass-ceramics. Especially, the band IV (~600 nm) is lacking in all borate glasses. This color center has been ascribed to Te_2^-. Murata et al.[9] discussed the NIR luminescence characteristics of various

Bi-doped glasses based on optical basicity concept without any reducing agents, and they reported that the generation of NIR luminescence was affected strongly by optical basicity of base glass. They concluded that Λ of 0.4 was the critical point (above 0.4 no NIR luminescence was observed). As discussed in the previous section, the concentration of the color center due to Te_2 or Te_2^- species might be very low, resulting in the lacking of absorption bands and NIR luminescence in all borate glasses. On the contrary, the Λ values for Te-SL and Te-Spinel are 0.58 and 0.47. These values are much larger than that of ZTP glass. However, a small amount of carbon was added into Te-SL glass, which was melted at a higher temperature (1450°C), and Te-Spinel glass was melted at a much higher temperature (1600°C). The reducing agent and higher melting temperature enhance the reducing condition, and hence it seems that Te-SL and Te-Spinel glass and glass-ceramics exhibited NIR luminescence.

Consequently, it is suggested that the origin of NIR luminescence of Te-containing glasses is likely to be caused by Te_2^-.

4. Conclusion

The effects of the melting temperature and glass composition on the Near-infrared (NIR) luminescent characteristics of Te-containing borate glasses are investigated and compared with previous works.

Three absorption bands are detected at around ~370 nm, ~430 nm and ~530 nm, however, the absorption band at around ~600 nm cannot be detected in all borate glasses. Also, no NIR luminescence was observed under the excitation of a 974 nm laser diode. The NIR luminescence was observed in Te-green and Te-purple glasses, which showed the absorption band at around ~600 nm. This absorption band was derived from $^2\Pi g \rightarrow ^2\Pi u$ transition of Te_2^-.

Consequently, it is suggested that the origin of NIR luminescence of Te-containing green and purple glass is likely to be caused by Te_2^- center. (As with abstract, not sure of the real meaning of the sentence...)

References

1) Y. Ohishi, A. Mori, M. Yamada, H. Ono, Y. Nishida and K. Oikawa, *Opt. Lett.*, 23, 274–277 (1998).
2) A. Mori, T. Sakamoto, K. Kobayashi, K. Shikano, K. Oikawa, K. Oshino, T. Takamori, Y. Ohishi and M. Shimizu, *IEEE J. Lightwave Technol.*, LT-20, 822 (2002).
3) Y. Hasegawa and S. Sakamoto, *Glastechn. Ber.*, 30, 332–335 (1957).
4) T. Konishi, T. Hondo, T. Araki, K. Nishio, T. Tsuchiya, T. Matsumoto, S. Suehara, S. Todoroki and S. Inoue, *J. Non-Cryst. Solids*, 324, 58–66 (2003).
5) G.-G. Lindner, K. Witke, H. Schlaich and D. Reinen, *Inorg. Chim. Acta*, 252, 39–45 (1996).
6) S. Khonthon, S. Morimoto, Y. Arai and Y. Ohishi, *J. Ceram. Soc. Japan*, 115, 259–263 (2007).
7) Y. Arai, T. Suzuki, Y. Ohishi and S. Morimoto, Proceedings of XXIst International Congress on Glass, July 1–6, Strausbourg, France, M6 (2007).
8) I. A. Duffy, *J. Non-Cryst. Solids*, 196, 45–50 (1996).
9) T. Murata and T. Mouri, *J. Non-Cryst. Solids*, 353, 2403–2407 (2007).

BIOGRAPHY

Penprapa Punpai was born on November 19, 1984 in Roi-Et Province, Thailand. She graduated in Bachelor Degree in Ceramic Engineering from Suranaree University of Technology in 2006. After graduation, she furthered the study for Master Degree, supported by Suranaree University of Technology, in Ceramic Engineering at School of Ceramic Engineering, Institute of Engineering at Suranaree University of Technology from year 2007 to 2009. During her Master Degree study, she had two paper presentations and two paper-published in international journals.